SLOVENSKÁ TECHNICKÁ UNIVERZITA V BRATISLAVE

FACULTY OF CHEMICAL AND FOOD TECHNOLOGY

MASTER THESIS – CHEMICAL ENGINEERING

THERMAL CHARACTERIZATION OF MSW FOR PURPOSE OF ITS GASIFICATION AND PYROLYSIS

ABEL VALVERDE SALAMANCA

UNIVERSITAT POLITÈCNICA DE CATALUNYA

Director: Prof. Ing. Jozef Markoš, DrSc. 2014

Contents

Summary

Due to the increase of municipal solid waste (MSW) as the population and their consume increase, new technologies of waste removal have to be developed, in order to find a MSW disposal method which do not fill lands and neither pollute the environment. Therefore, pyrolysis is raised as a way of MSW removal which at the same time can produce profitable products. This thesis is aimed at measuring the yields obtained from a pyrolysis process from different MSW mixtures, as well as the influence of temperature on the product yields is determined. For this purpose, a characterization of MSW components and the resulting products has been carried out by means of thermogravimetric, calorimetric and elemental analyses.

After a quick introduction to the MSW production as well as the nowadays technologies of removal, the description of the equipment used during experimentation and discussion of results, the thesis arrives to final conclusions, where an overall view of the results is done.

Keywords: municipal solid waste (MSW), pyrolysis, gasification, high temperature, degradation, tar, ashes, volatile fraction, thermogravimetric analysis, calorimetric analysis, elemental analysis, gas chromatography (GC).

Acknowledgments

This thesis couldn't have been possible without the help of some people, who have been supporting and contributing with their advices, knowledge and material support all throughout the thesis:

Ing. Jozef Markoš, DrSc. – For his help and advice during the elaboration of the thesis and especially for the starting support which structured in the best way this thesis.

Doc. Ing. Juma Haydary, PhD. – For his help in the experimentation and providing the aim of the thesis as far as advices for the research of it.

Ing. Dalibor Susa – For his continuous help all along this thesis, providing documentation, experimental data, advice, constant supervision and availability in any moment, and for his final revision of the work. This thesis couldn't have been completed without his help.

And lastly I would like to thank fellow Slovak students Miroslav Mrva and Viktor Gelinger for their help in laboratory.

1. Introduction

1.1. Background

As years go way, the demand of energy increases, and becomes clearer the need to search for new sources, renewable and non-polluting. That is the reason why in these last years the development and research on renewable sources of energy is coming more and more significant.

Lately many power plants have been built where the radiation of the sun is used to generate electricity. It can be solar thermal plants, where the heat from the sun is taken by panels that increase the temperature of the water that is circulating in pipes through the panels in order to achieve the amount of steam needed to drive a turbine. On the other hand, there are the photovoltaic solar plants, where the radiation of the sun is directly converted into electricity by means of a panel made of semiconductor. Nevertheless, this technology is only able to achieve the efficiency of 15% and a 20% (Schultz et al., 2007), and taking into account that the average of sun radiation that receives the panel is 1000 W/m^2 a huge economical investment is needed in order to generate a considerable amount of energy.

The wind is another way to generate electricity in a renewable and non-polluting way. It consists in large amounts of aeolian generators called wind farms, placed there after an exhaustive study of the strength of the wind and its flows, which are capable to convert the kinetic energy that the wind carries into a rotating movement of the blades, that is translated to the rotating movement of the axis which generate the electricity inside the generator. These kinds of generators have a quite good efficiency as it is between a 20% and a 45%, but it is very variable as it depends on the wind speed (SAEM Thales, 2001). Furthermore, the worst inconvenience is this variability of the wind, since it is not possible to control the amount of energy that is generated. Moreover, there are a lot of critics against the visual impact it has on the landscape, and the damage to some animal species like birds.

Nowadays, one of the most used renewable energies used is the hydropower. It consists in taking profit of the energy of the water (either kinetic and pressure energy), in order to drive a turbine that transmits the mechanical energy to the axis, and finally electricity is obtained in the generator. It can be a different plant depending on the site of the plant:

- Dam plant: These are the conventional plants where in a huge river dam is built in order to create enough head so the turbine can work. Depending on the head and the flow one kind of turbine is used (axial Kaplan for high flow and low head, radial Francis for quite high head and low flow, and Pelton for very high head and low flow). This kind of plants cannot store water once it passes through the turbine.

- Pumped-storage plants: These kind of plants are located between two reservoir of water (usually artificial), and the equipment used is a hybrid turbine and pump machine, or separate pump and a turbine, in order to work like a turbine when electricity is required, and work like a pump when there is excess of electricity in the network, so it can take profit of it pumping water to the upper reservoir and storing it. These plants are very useful, as they can store energy and give electricity when it is needed.
- Run of the river plants: These are plants sited in the run of the river, where is made a small head, and the water is derived to a turbine, usually a horizontal Francis.
- Marine plants: There are plants focused on taking profit of the marine water energy. The turbines usually are axial Kaplan or Bulbo, and the aim is to use either the strength of the marine water, the currents or the waves of the sea to generate electricity. These kinds of plants are not very used as the sea water is very corrosive and the turbines and the pipes need a lot of maintenance and there is not a huge amount of energy taken from it.

The efficiency of hydropower plants is between 65% and 90% (Islam et al., 2011), so is one of the most efficient methods to generate electricity in a renewable and non-polluting way. It needs a strong economical investment, due the need of a huge civil build, and an expensive apparatus and maintenance, but it is very profitable.

1.2. Municipal Solid Waste (MSW)

Following the same target as the renewable energies that has been explained, it is possible to obtain energy from the items that everyday each person discards; those are the Municipal Solid Waste (MSW). This way, it is possible to use a renewable energy method that moreover reduces the amount of waste produced which is increasing every day.

1.2.1. Composition and disposal of the MSW

The composition of MSW usually contains biodegradable waste, such as food waste, wood and paper (also recyclable*);* recyclable material, as paper, glass, cans, clothes, some plastics, etc.; Inert waste as sand, rocks, etc.; plastics not able to be recycled; hazardous and toxic waste, such as chemicals, paints, light bulbs, spray cans, herbicides, pesticides, etc.; and medical waste (EPA, 2012). Nevertheless, the exact composition depends on the region it comes from, so in a developed country recycling culture the main formers of the MSW are wastes not able to be recycled like plastics, but in a non-recycling culture the waste can contain a lot of food waste, paper, etc. The MSW do not include industrial waste, neither agriculture waste, or radioactive waste, etc.

In the following figure it can be seen the MSW composition by region.

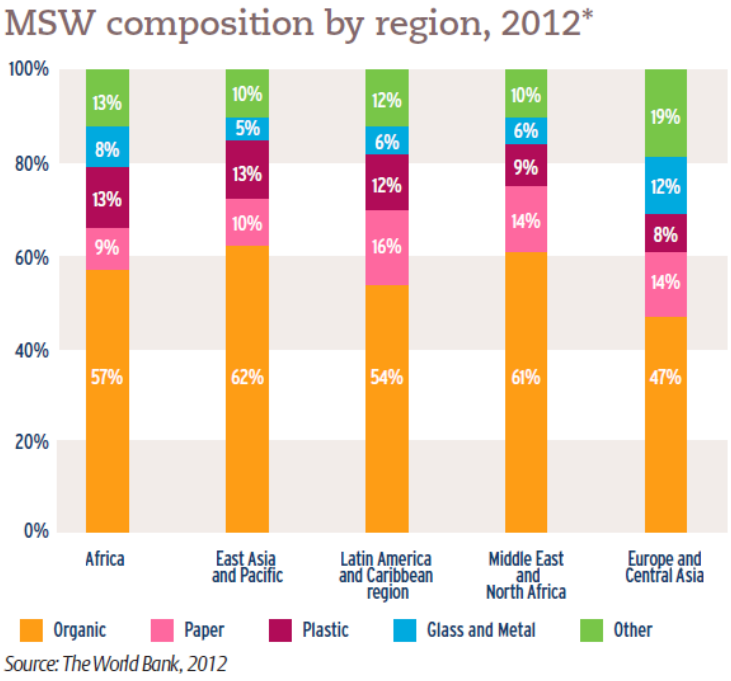

Figure 1. MSW composition by region (Popraco, 2012, Source: The World Bank, 2012).

In Figure 1 it can be seen how for example in Europe there is less organic waste (47%) than the others, maybe for its recycling culture, and more glass, metal and others (31%); and in Africa the waste consists of more organic items (57%) in comparison with the other non-recyclable wastes.

The disposal of the MSW is different and also depends on the region it comes from as well as technological development, economic situation, type of waste, etc.

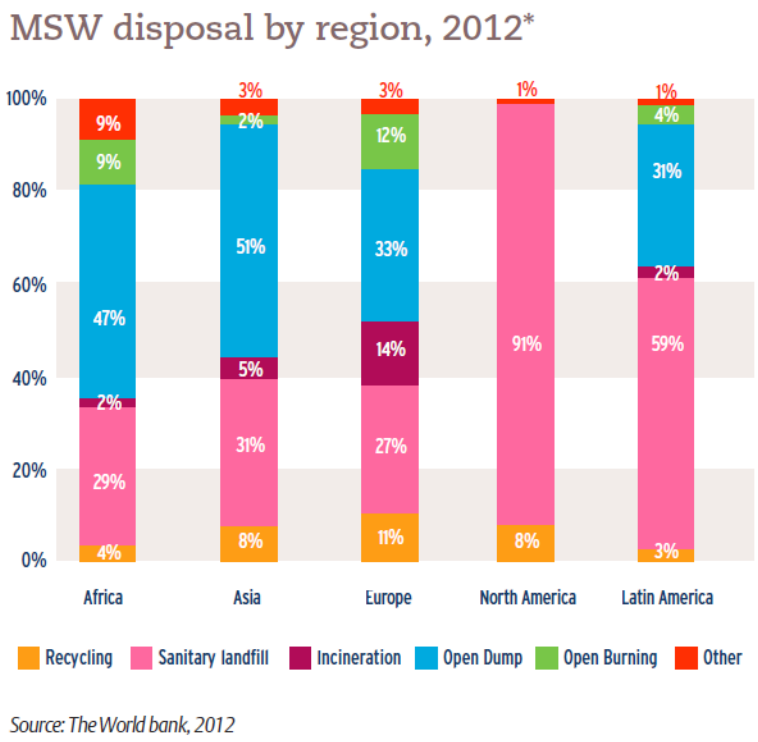

Figure 2. MSW disposal by region (Popraco, 2012, Source: The World Bank, 2012).

In Figure 2 it is easy to see the difference between the disposal depending on the continent, as in Europe there is more recycling (11%) and incineration (14%) and less dumping (33%), in Asia there is more dumping (51%) and less recycling (8%). It is interesting too, how in North America the 91% of the waste is disposed for sanitary landfill, maybe because there is the enough space for it, and they have followed these politics since a long time.

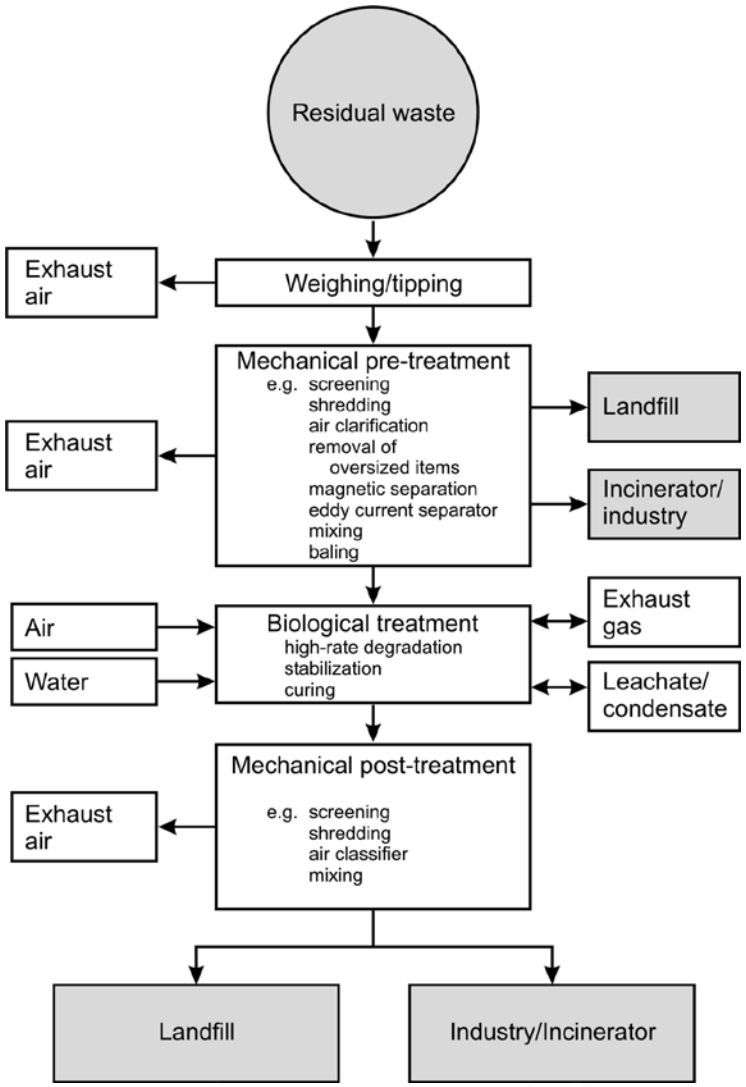

Figure 3. Pre- and post-processing of MSW to produce stable products (Christensen et al., 2011).

Figure 3 is a scheme about the pre-processes and post-processes which MSW can undergo. It is easy to see the significant number of processes which MSW must undergo in order to take profit of it. The main three final destination processes for MSW are thermal treatments (including incineration, pyrolysis and gasification), biological treatment and landfilling.

1.2.2. Biological Treatment

The aerobic degradation of solid organic matter is called composting. Composting happens spontaneously in the nature as the plant litter, animal residues and manure is decomposed. The same spontaneous process can be forced and accelerated in order to degrade the waste by microbial activities in aerobic conditions and in solid state. The process is exergonic, so it releases more energy than it takes. About 50% and 60% of this energy is used by microorganisms to synthesize ATP, and the other is lost as heat, which behaves an increase of the temperature. On the first phase of composting, the easily degradable organic matter is first decomposed in a mesophilic process (temperatures around 15 and 35ºC) and the mass of material quickly decrease therefore

a huge amount of energy is released in form of heat, which behaves a temperature and degradation rate increase. Few days after this first part, the increase of temperature leads to a thermophilic phase, where the microorganisms in the process can bear extreme temperatures. Now the temperature can reach 70ºC, which in controlled composting is limited, in order to obtain high stabilization rates as well as good sanitization. After, starts the third phase, maturation, where slowly degradable molecules undergo a mineralization and lignocellulosic compounds undergo humifictation. During composting process, intermediate metabolites can lead to a phytotoxicity of the composting material, which is overtaken at the end of the process and the final product is beneficial to the plant growth. Is important to finish the process just after phytotoxicity is removed, because if it goes on too long the final product loses beneficial proprieties, which are related to the production of carbon dioxide, water, minerals and biologically stabilized organic matter. The final product from composting process is called compost. The process is a batch process where the microorganisms needed are usually already on the material when the process starts, and if they are not, the microorganisms must be inoculated (Christensen et al., 2011).

Figure 9 represents the different stages of composting process by the oxygen consumption during the composing.

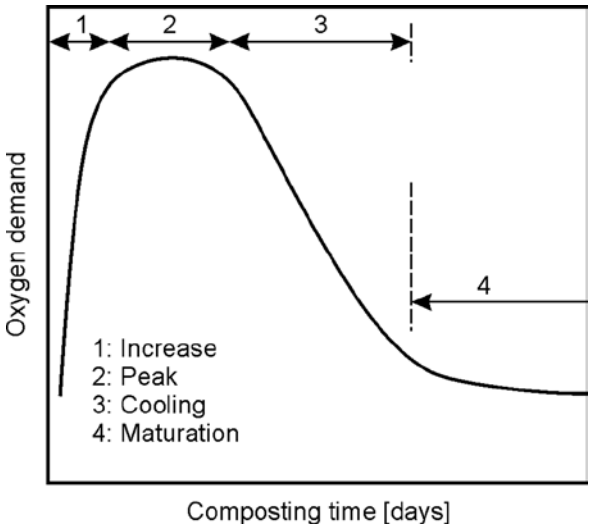

Figure 9. Oxygen consumption curve during composting (Christensen et al., 2011).

There are two kind of compost that needs to be distinguished: stabilized compost, compost after it has passed through the first stage of biooxidation; and mature compost, which is the compost that has been stored a long time in order it has undergone a substantial humidification (Christensen et al., 2011).

The total amount of heat that can release composting process is approximately 19 MJ/kg dry matter degraded (Christensen et al., 2011).

Benefits	Drawbacks
Saleable Product	Loss of ammonia (N)
Destruction of pathogens	Time involved
Kills weed seeds	Cost of equipment
Reduces mass and volume	Land required
Improved handling	Marketing required for sale
Improved transportability	
Soil conditioner	
Reduces odor	
Land application when convenient	
Improves nutrient qualities	
Decreases pollutants	

Table 8. Benefits and drawbacks of composting (Nelson, 2002).

Table 8 explains the benefits and drawbacks of composting. Comparing to thermal treatments as incineration and pyrolysis and gasification, composting requires a lot of land, that with the facilities that have to been built, it needs a high economical investment and a lot of land to do it. Moreover, it's not possible to get the same gas production as in thermal treatments, and the energy produced is less. Nevertheless, the advantage is that composting is more easy technology and more improved than pyrolysis and gasification for example.

1.2.3. Landfilling

The most used route for waste management in history has been landfilling, and still it is in many countries. Although landfill technology has developed a lot until now, with more control measures and highly engineered facilities, it is still based on waste accumulation for a long time in the environment which produces several problems with which engineering has to deal. One of the solutions for landfilling has been isolation of the waste in order to prevent polluting emissions. Nevertheless, isolation accumulates emission so it can be more dangerous if the isolation fails after long time (Christensen et al., 2011).

Landfilling is a much discussed measure for waste disposal because of its polluting potential. Waste in landfills can attract new fauna and flora to the surroundings and also repelling the surrounding fauna and flora. Furthermore, landfills can produce polluting emissions to air and leachates to the soil and water. Therefore, before the implantation of a new landfill, a lot of research has to be done, like what kind of waste will be in it, geological and hydrological studies, which landfilling technology to use, which technical environmental protection measures to take, etc. Although modern landfills can avoid most of environmental impacts, it is still dangerous.

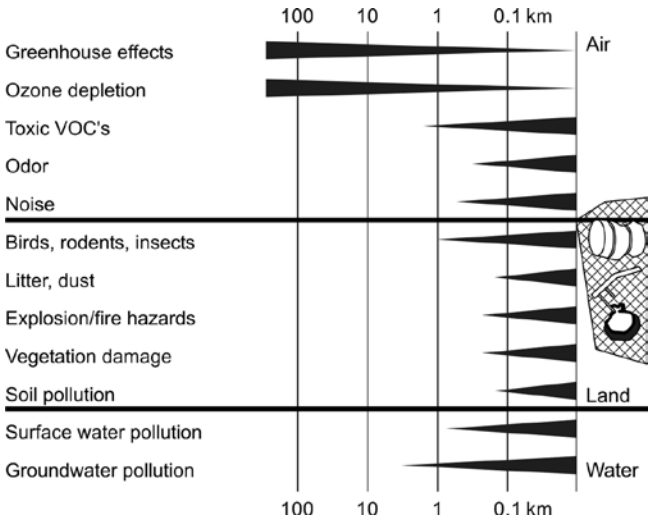

Figure 10. Potential environmental impacts with estimated zone of influence of each potential impact (Christensen et al., 2011).

In Figure 10 the potential environmental impacts that landfills can produce are displayed. There are two which are global impacts: greenhouse effects and ozone depletion. The others are more or less local impacts.

Compared to other thermal treatments such as incineration, pyrolysis and gasification, landfilling is cheaper solution, but the gasses emitted by the landfill are usually less profitable, neither the heating value of wastes. Moreover, landfilling generates more environmental problems than thermal treatments as there is a reduction of greenhouse gas emissions from anaerobic decomposition of the organic wastes (it has been estimated that about 1 ton of equivalent CO_2 is saved per each ton of waste combusted rather than landfilled (Psomopoulos et al., 2009) and it needs a large area of land. Furthermore it does not remove the waste, just store it, so everyday more land will be needed (a waste-to-energy (WtE) plant processing 1 Mt/y for about 30 years is estimated to require less than 100000 m^2 of land compared with the approximately 3000000 m^2 that would be necessary for landfilling of 30 Mt of MSW) (Psomopoulos et al., 2009).

1.2.4. Thermal Treatment

In order to get energy from the Municipal Solid Waste, there are different thermal treatments that can be carried out. Each one of those has its advantages and disadvantages. In Table 1 the main characteristics and differences of each thermal treatment are presented.

	Incineration	**Gasification**	**Pyrolysis**
Aim of the process	To maximize waste conversion to high temperature flue gases, mainly CO_2 and H_2O	To maximize waste conversion to high heating value fuel gases, mainly CO, H_2 and CH_4	To maximize thermal decomposition of solid waste to gases and condensed phases
Operating conditions **Reaction environment**	Oxidizing (oxidant amount larger than that required by stoichiometric combustion)	Reducing (oxidant amount lower than that required by stoichiometric combustion)	Total absence of any oxidant
Reactant gas	Air	Air, pure oxygen, oxygen-enriched air, steam	None
Temperature	Between 850ºC and 1200ºC	Between 550-900ºC (in air gasification) and 1000-1600ºC	Between 500ºC and 800ºC
Pressure	Generally atmospheric	Generally atmospheric	Slight over-pressure
Process outputs **Produced gases**	CO_2, H_2O	CO, H_2, CO_2, H_2O, CH_4	CO, H_2, CH_4 and other hydrocarbons
Pollutants	SO_2, NO_x, HCl, PDD/F, particulate	H_2S, HCl, COS, NH_3, HCN, tar, alkali, particulate	H_2S, HCl, NH_3, HCN, tar, particulate
Ash	Bottom ash can be treated to recover ferrous (iron, steel) and non-ferrous metals (such as aluminium, copper and zinc) and inert materials (to be utilized as a sustainable building material). Air Pollution Control residues are generally treated and disposed as industrial waste	As for combustion process. Bottom ash are often produced as vitreous slag that can be utilized as backfilling material for road construction	Often having not negligible carbon content. Treated and disposed as industrial special waste
Gas cleaning	Treated in air pollution control units to meet the emission limits and then sent to the stack	It is possible to clean the gas to meet the standards of chemicals production processes or those of high efficiency energy conversion devices	It is possible to clean the gas to meet the standards of chemicals production processes or those of high efficiency energy conversion devices

Table 1. Main characteristics of the chemical process for thermal treatment of solid waste (Arena and Mastellone, 2009).

1.2.4.1. Incineration

Incineration is a thermal treatment that has been done for a lot of years, evolving from a basic incineration in the disposal site to modern efficient plants with process and emission control systems.

Waste incineration is a thermal conversion of waste with a surplus of air. The process releases energy and also it produces solid residues and gas which are emitted to the atmosphere. One of the most important differences between the other combustion systems is the great variety of composition that the incineration can bear, and this is very important when the design of the incineration plant is done. However, when the real design is carried out, there are limits to the variation of the waste composition it can allow, therefore a big amount of data about the composition of the waste is needed taking into account the possible variation of the composition in the future. The design of the furnace also depends on the heating value of the waste that must be obtained before with calorimetric experiments (Christensen et al., 2011).

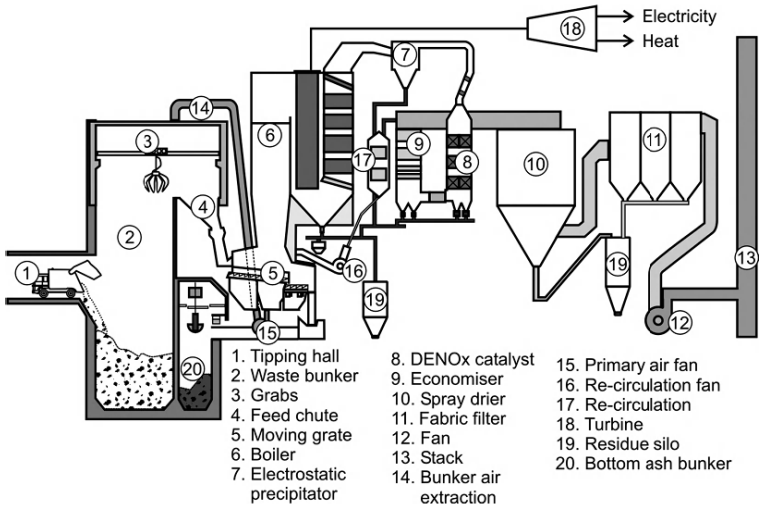

Figure 3. Cross-section of a typical waste incineration plant with a moving grate furnace (Christensen et al., 2011).

Figure 4 is a cross-section of a typical waste incinerator with a moving grate furnace and a steam boiler so it generates both electricity and heat. The result inside the furnace is the reaction between the combustible components and the oxygen of the air releasing hot combustion gas. During the incineration process, the waste undergo several different processes like drying, pyrolysis and gasification (where the combustible gases are emitted), ignition and combustion of the combustible gases, and the final burn out of the solids leaving only char and ashes. For a complete burnout it is needed to maintain a temperature in the afterburning chamber about 850º for MSW during minimum 2 seconds. It is important also in order to reduce the amount of CO that is emitted to the atmosphere since a low temperature of combustion, a lack of oxygen or too short time residence can lead to limit values of CO.

The composition of the flue gases is a good indicator of the efficiency of the incineration plant. The electricity generation is based on a Rankine process, which leads

to an efficiency between 20% and 25% for the thermal process, and between 25% and 35% for the power generation (Christensen et al., 2011).

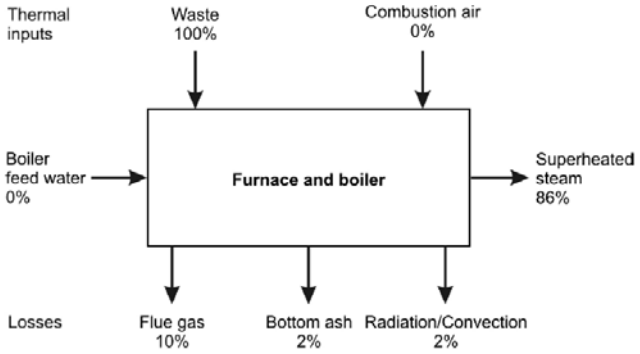

Figure 4. Energy balance of the furnace/boiler with typical values (Christensen et al., 2011).

Figure 5 is a flow diagram about the energy balance on the furnace and boiler of the incineration plant. In it can be seen how an 86% of the waste energy is used for generating steam in order to generate electricity in the turbine, a 10% will be emitted as flue gas, 2% is lost by radiation and convection, and only a 2% will be ashes. The waste are reduced a 90% in volume, and between a 70% and 80% in mass.

Incineration is an argued method in the society since in some countries it is seen like a way to eliminate waste and generating power, but in some others it is seen like another way of producing energy by polluting the atmosphere and endangering the public health.

1.2.4.2. Co-combustion

Co-combustion or co-incineration is the name given to the use of combustible wastes in industrial combustion facilities that are not focused on the waste treatment of waste but they have to provide thermal energy or electricity to a process, and usually use fossil fuels for it. Those wastes used just for recovery energy in industry are often called refuse-derived fuel (RDF) or solid recovered fuel (SRF).

The advantages of using this method are basically three:

- **Cost reduction**: Some combustible wastes have similar heating value than common fossil fuels like oil or coal, but are cheaper.
- **CO_2 reduction**: Some wastes can be renewable.
- **Diversified fuel market**: Using wastes an industry can reduce the dependence on a certain fuel and the prices it has in the market.

Nevertheless, the use of combustible wastes in the industry must be controlled since there are some chemicals that need to be removed first from the waste, as Cd, Zn and Hg, which are dangerous for human either for the facilities. Moreover, its use can behave increased pollution without a good air pollution control, corrosion of the equipment because of Cl and S, damage for the catalysts, instable process, etc.

Nowadays cement kilns, blast furnaces, pulp and paper mills, drum mixer asphalt plants, ceramic manufacturers, lime works, coal-fired power plants, biomass-fired boilers, etc., are using this technology. Usually, between 10% and 20% of the energy input are substituted by waste, but it seems that this percentage can even reach the 70% (Christensen et al., 2011).

1.2.4.3. Pyrolysis and gasification:

Those two processes are focused on converting solid materials by thermal treatment yielding three types of products like gas, char and liquid. Pyrolysis usually generates more products such as gas, tar and char, and gasification converts the materials containing carbon into mainly gas, this is the reason why gasification is often used after pyrolysis, using as inputs the outputs of pyrolysis in order to obtain more gas (useful for heating and other applications) and less ash, char, coke and tar. However, pyrolysis can be carried out without need of gasification. Therefore the output composition depends not just on the method, but also on the configuration of the experiment and the composition of the feed.

Gasification has been done for a long time. In the 19th century gasification of coal was used in order to generate gas for applications as illumination. During the World War II, in Europe appeared wood-fueled gasifiers, known as gas generators, due to the run out of oil-based fuels. And between 1970s and 1980s, with the oil price crisis, the gasification technology evolved in order to find a cheaper substitute of oil-based products by means of gasification of coal. Nowadays, the most significant application of gasification is aimed to produce H_2 and CO rich gas from coal, in order to use it as chemical feedstock or energy production; nevertheless, the use of biomass and MSW gasification is gaining interest so it can be found new technologies for sustainable energy, although it is still few significant in front of the other applications. The reason why pyrolysis and gasification of MSW is becoming more important is the difficulty for some countries to build incineration plants, which require a high economical invest, and the advantage to preserve better the energy of the waste (Christensen et al., 2011).

In Table 2 the benefits and drawbacks of pyrolysis and gasification with respect to incineration are explained.

Benefits	Drawbacks
Recover of chemicals such as hydrogen and other chemical feedstock rather than converting the chemical energy of waste into hot flue gasses.	The input fuels need some homogeneity, so if the feedstock doesn't reach the required homogeneity, it must be pretreated and homogenized.
Better energy efficiency.	The control of the process is complicated and there can be troubles with slugging, tars and contaminants.
Less corrosion.	
Less need to clean the flue gases since they have smaller volume and have better quality.	The use for pyrolysis and gasification for MSW has only been demonstrated for small scale and for specific fuel types, so it is needed a careful review of the technology to use for a specific waste mix, facilities, etc.
Better CO_2 capture.	
Lower emissions of dioxins.	
For high-temperature processes, solid residues have more quality.	Nowadays, energy conversion efficiencies obtained with pyrolysis and gasification cannot compete with modern waste incinerators.
As gasification units work with low load, it is possible to build small gasification plants producing less than 1 MW.	
Lower cost.	

Table 2. Benefits and drawbacks of pyrolysis and gasification with respect to incineration. (Juniper, 2001; Klein et al., 2002; Malkow, 2004).

The process of pyrolysis and gasification include a wide range of operations with complex heterogeneous and homogeneous reactions. As has been said before, pyrolysis and gasification are different processes despite being very similar, as they have mainly difference in the gasification agent and the processing temperature. Nevertheless, they are often combined, carrying out first pyrolysis process connected to the following gasification process, as can be seen on Figure 6.

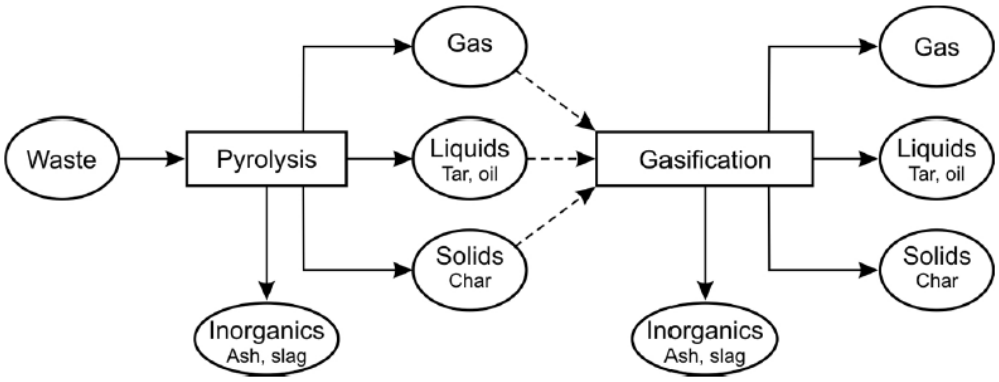

Figure 6. Scheme of pyrolysis and gasification including an outline of the outputs (Christensen et al., 2011).

As it is drawn in Figure 6, pyrolysis and gasification do not have to be connected, although usually gasification includes heterogeneous reactions using the outputs from pyrolysis.

- **Pyrolysis**

  During pyrolysis process the organic material undergo a thermal degradation in absence of oxidizing agents as oxygen, steam, and CO_2. The typical temperatures are between 300 and 800 ºC (Christensen et al., 2011). Although it is an endothermic process, so in order to the process proceed energy is required.

  The energy that products contain and its composition depends on the MSW input characteristics, so they can vary significantly depending on the input. Table 3 summarizes the main products obtained:

Product	Composition	Definition
Gas	Mainly hydrogen (H_2), methane (CH_4), carbon monoxide (CO), carbon dioxide (CO_2), and other volatile components of the MSW.	Between 20% and 50% by weight of the input. Approximate heating value around 3-12 MJ/Nm^3.
Liquid	Tar, oil, and water containing complex hydrocarbons such as organic acids, phenols, polycyclic aromatic hydrocarbons (PAHs), and alcohols.	The aqueous phase can be a considerable part of the liquid. Between 30% and 50% by weight. Approximate heating value around 5-15 MJ/kg.
Solid	The remaining part of products are solids similar to char containing metals, sand, glass, etc.	The char can be around 20% and 50% by weight, which can contain between 10% and 50% of ash. Approximate heating value around 10-35 MJ/kg.

Table 3. Summary of products from pyrolysis process (Juniper, 2001; Williams, 2005).

The values in Table 3 are just indicative values for general well-sorted refuse derived fuel, automobile waste, or biomass waste. If the waste input has more quality (well-sorted waste), higher ratios of oils and gasses will be obtained; but if the input waste is mixed, it can produce more char and solid residues (inorganic residues). The water present in the waste is also influential, particularly for the gas and liquid products.

The pyrolysis process is divided into different phases. In the first phase the moisture is released from the waste by drying it at 100-120ºC. After this phase, volatile compounds are released and the compounds with complex carbon strings are degraded to more carbon simple strings by a series of complex reactions. As the temperature increase from 200ºC to 800ºC, oxygen, hydrogen and nitrogen bonds are broken, so the gaseous outputs are formed; these are the primary reactions (Bilitewski et al., 1997). The secondary reactions take place after these primary reactions, where the tar can be converted into more gases and char, as well as there is an increase of CO_2 and CH_4 generation. Secondary reactions are also carried out in gasification process. The pyrolysis reactor is heated through the walls although compaction of the waste and friction also contribute to heating. Pyrolysis is said to be held in an inert atmosphere, but the reality is that it takes place into a pyrolysis gases atmosphere that generate some secondary conversion reactions.

Temperature Range (ºC)	**Chemical Reactions**
100-120	Thermal drying, dehydration.
250	Deoxidation, desulfurization, molecular splitting of water and carbon dioxide, splitting of hydrogen sulfide.
340	Breakage of bonds of aliphatic compounds, splitting of methane and other aliphatic compounds.
380	Carbonization
400	Breakage of carbon-oxygen and carbon-nitrogen.
400-600	Decomposition of bituminous compounds into low-temperature oils and tars.
600	Cracking of bituminous compounds into heat resistant components (gaseous, short-chained hydrocarbons), formation of aromatic compounds (benzene and derived compounds).
>600	Olefin (ethylene), reaction of ethylene to cyclohexane, thermal aromatization to benzene and higher-volatility aromatic compounds.

Table 4. Pyrolysis reactions as a function of the temperature (Bilitewski et al., 1997). Reprinted with permission from Waste Management by B. Bilitewski, G. Hardtle, K. Marek et al., XV 9783540592105©(1997) Springer Science + Business Media.

- **Gasification**

During gasification process, the organic material undergo a thermal and chemical conversion into a mainly gaseous output by means of partial oxidation in presence of a gasification agent, that usually is air, steam or oxygen. When gasification is used after pyrolysis, the inputs of the process are the outputs of pyrolysis (gas, tar and char), so they can be upgraded by partial oxidation of the complex hydrocarbons contained in tar and char. The ranges of temperatures of

operation during the gasification process are between 800ºC and 1100ºC when air is used as oxidation agent and up to 1500ºC when it is oxygen (Christensen et al., 2011). Although gasification is an exothermal process, endothermic reactions are involved in it so they need heating that can be supplied for example from the steam when it is the gasification agent. In Table 5 the products of gasification process are explained.

Product	Composition	Definition
Gas	Similar to the gas obtained in pyrolysis but with a higher content of carbon dioxide (CO_2).	Between 30% and 60% by weight of the input. Heating value depends on the gasification agent, but it is approximately around 3-12 MJ/Nm^3, higher with oxygen as gasification agent.
Liquid	Smaller quantities of tar and oil.	Between 10% and 20% by weight of the input. Approximate heating value around 5-15 MJ/kg.
Solid	Mainly ashes containing metals and other inorganic components.	Ashes can be around 30% and 50% by weight of the input. Approximate heating value around 10-35 MJ/kg.

Table 5. Summary of products from gasification process (Juniper, 2001; Belgiorno et al., 2003; Williams, 2005).

The waste input, temperature of operation and the configuration of the process are very influential in the gasification products. The produced gas composition also like its heating value is highly dependent on the gasification agent used. The heating value of the gas output is affected by dilution from the gasification agent. For example, using air as gasification agent is cheaper than using oxygen, but the resulting gas can contain up to 60% of nitrogen (Juniper, 2001). So as gasification can be discriminated depending on the gasification agent: indirect gasification, when there is not an oxidizing agent, like steam (Hauserman et al., 1997; Staniewski, 1995), and direct gasification if the process takes place with an oxidizing agent like air or oxygen. This difference can be seen in Figure 7.

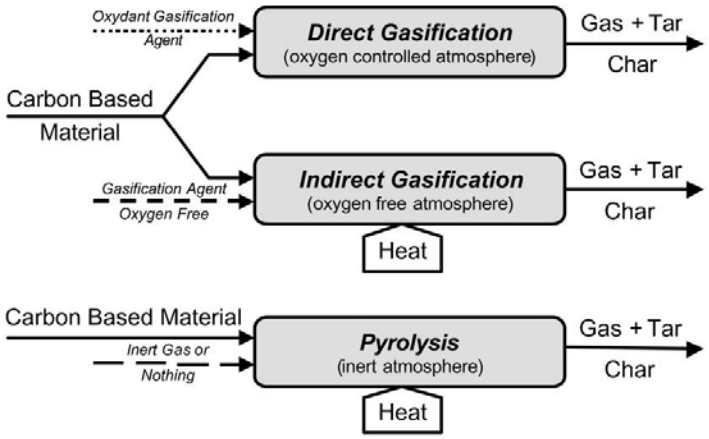

Figure 7. Types of gasification depending on the gasification agent (Belgiorno et al., 2003).

In the indirect gasification there is a low gas production rate that reduces the cost of energy recovery and gas cleanup systems but it is a complex process and increases investment costs (Hauserman et al., 1997).
Direct gasification with oxygen as the gasification agent has the same advantages as indirect gasification, but the use of pure oxygen is expensive as its cost can reach more than 20% of the overall electricity production (Della Rocca, 2001). On the other hand, direct gasification with the presence of nitrogen, taking air as gasification agent, reduce the volumetric efficiency and produce a gas with lower heating value (De Feo et al., 2000; Paisley, 1998).

The main advantage of carrying out gasification process after pyrolysis is that by operating at higher temperatures and adding a gasification agent, pyrolysis products such as tar and char are further converted to CO, CO_2, H_2 and CH_4 (Juniper, 2001).

Reactions involved in pyrolysis and gasification process are several and complex. In Table 6 there are the most important reactions that take place during pyrolysis and gasification process.

	Description	Reaction energy (kJ/mol)	Effect of temperature increase	Effect of pressure increase
Solid-gas reactions				
$C + 1/2O_2 \rightarrow CO$	Partial combustion	110.6	To right	To left
$C + O_2 \rightarrow CO_2$	Combustion	393.8	-	-
$C + 2H_2 \rightarrow CH_4$	Hydrogenation	79.9	To left	To right
$C + H_2O \rightarrow CO + H_2$	Water -gas	-131.4	To right	To left
$C + CO_2 \rightarrow 2CO$	Boudouard	-172.6	To right	To left
Gas-gas reactions				
$CO + H_2O \rightarrow CO_2 + H_2$	Shift	41.2	To left	-
$CO + 3H_2 \rightarrow CH_4 + H_2O$	Reforming	201.9	To left	To right
Secondary solid-gas reactions				
$Tar + H_2O \rightarrow CO + H_2$	Steam reforming	-	-	-
$Tar + H_2 \rightarrow$ hydrocarbons + gas	Hydro cracking	-	-	-
Tar + catalyst → char + gas	Cracking	-	-	-

Table 6. Important pyrolysis and gasification reactions (partly based on Juniper, 2001). Adapted from Pyrolysis and Gasification of Waste: A Worldwide Technology and Business Review © (1997) Juniper Consultancy Services.

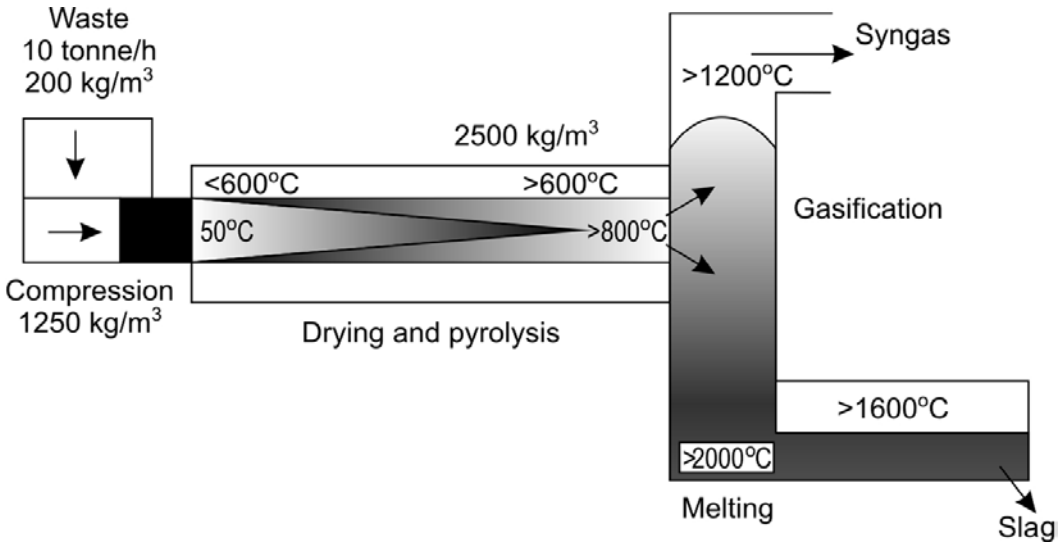

Figure 8. Example of pyrolysis and gasification plant. This is a scheme of Thermoselect process for treatment of MSW, which was tested in a demonstration plant in Italy and after was build the first commercial plant in Karlsruhe (Germany) in 1999 with capacity 225000 t/year (Christensen et al., 2011).

Nowadays there are some companies in the world that use pyrolysis and gasification process to obtain energy in a commercial plant. Some of them listed in Table 7.

Company	Description
Compact Power (UK)	Pyrolysis and gasification with oxidizing agent is used in order to convert waste into fuel and coal. It can take an input of 8000 tonnes of waste a year.
Shanks (UK)	Is developing bio-drying with gasification, which uses bacteria to heat and dry waste. It has 50 MW installed on fluidized bed gasifiers.
Kemestrie (Quebec)	It has developed the technology called Biosyn, based on fluidized bed gasification. It treats 90% of organic waste.
Organic Power (Norway)	This Norwegian company has 8 projects to build in Scandinavia and South Korea small plants using combination of gasification and pyrolysis.

Table 7. Example of some companies that are applying pyrolysis and gasification in waste treatment (Friends of the Earth, 2002).

1.3. Pyrolysis and Gasification Technology

There are several different kinds of pyrolysis and gasification technologies worldwide as there are many manufactures with their own specific varieties. Nevertheless, those different technologies can be divided in two main groups whether the technology is focused on energy recovery, in order to produce gas with high content of H_2 and CO which can be used in gas motor, gas turbine or combustion boiler; or if the technology is focused on material recovery, in order to produce a stable solid residue that can be used in construction works or produce H_2 and CO rich gas used as chemical feedstock. Often material recovery occurs at the expense of energy recovery (Christensen et al., 2011).

Otherwise, reactor system can be also divided into two different kinds depending on the stages involved. It can be a one-stage process, as it uses only pyrolysis or gasification, usually when there is an homogeneous feedstock such as biomass and industrial waste fractions with a small variation of either physical and chemical characteristics over time. Nevertheless, when the main objective is to achieve better gas characteristics (more H_2 and CO content) or residue properties, or when the feedstock is a complicated mix as municipal solid waste, usually it is employed a two-stage process. It means a first stage of pyrolysis followed by a second stage of catalytic pyrolysis or gasification in a second reactor.

A brief description of pyrolysis/gasification reactors (for pyrolysis the rectors are the same but no gasification agent like air, oxygen or steam is introduced) used for MSW is reported in the following.

1.3.1. Fixed bed gasifiers (updraft and downdraft)

A deep bed of waste is present in almost all the volume of the reactor in a fixed bed gasifier, and there are different zones inside the reactor depending on the direction of the MSW flow and the gasification medium flow. Depending on the direction of the flow the reactor can be updraft or downdraft.

1.3.1.1. Updraft reactors

Here the waste moves counter-currently to the gases as the waste is fed in at the top of the gasifier and the gasification agent at the bottom. The waste passes through different zones while it circulates to the bottom (drying, pyrolysis, reduction and oxidation) until the outputs (ash and solid residues) are collected at the bottom. The gasifier is configured as cylinder shaped reactor mounted vertically. The off-gases (methane and tar-rich gas) are collected at the top (Christensen et al., 2011; Arena, 2011).

The main benefits of this kind of reactors are the simplicity of the construction and the thermal efficiency, as gas flow heat the reactor while they are circulating upwards the reactor. Drawbacks are the high tar production, the carryover of dust with the gas, slagging, and the difficulty of thermal control in each different zone inside the reactor (Christensen et al., 2011).

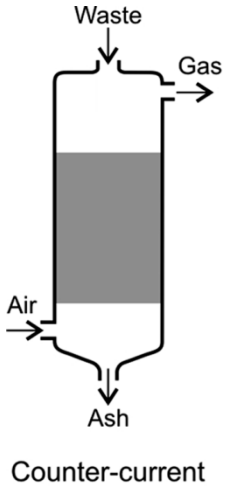

Figure 11. Schematic overview of updraft reactor (Christensen et al., 2011).

There are several plants in Japan, Germany and Italy.

1.3.1.2. Downdraft reactors

Downdraft reactors are similar to updraft reactors with the difference that the gasification agent is introduced into the reactor at the top or the sides, therefore waste and gases move co-currently towards the bottom of the gasifier. There are the same zones as for updraft gasifiers inside the reactor but in a different order. The ash is collected at the bottom of the gasifier, under the grate, and the gases leave at the base (Christensen et al., 2011; Arena, 2011).

The most significant benefit of this kind of gasifier is the reduction of tar obtained, caused by the circulation of the gasification agent through the hot char bed created in the high-temperature oxidation zone before leaving the gasifier. Moreover, this benefit involves a lower requirement of gas cleaning. However, in downdraft reactors clogging is easier, so it needs an accurate study of geometry (Christensen et al., 2011).

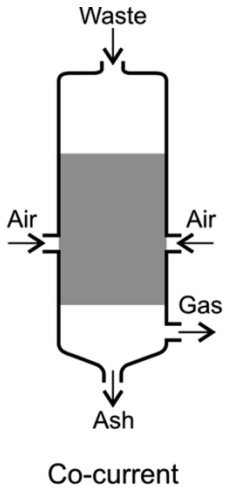

Figure 12. Schematic overview of downdraft reactor (Christensen et al., 2011).

There are several plants using this technology in Japan and Korea, constructed by Nippon Steel.

1.3.2. Fluidized bed gasifiers

In fluidized bed gasifiers the solids are kept 'in motion' but retained within the reactor. The benefits toward fixed bed gasifiers are the much better mixing and heat transfer. Therefore, there is a better uniformity in bed conditions and more conversion efficiency. Fluidized bed reactors are better for scale-up (Christensen et al., 2011).

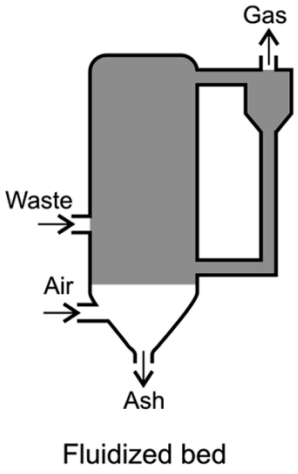

Figure 13. Schematic overview of fluidized bed reactor (Christensen et al., 2011).

There are two different kind of fluidized bed gasifiers: bubbling fluidized bed (BFB) and circulating fluidized beds (CFB).

1.3.2.1. Bubbling fluidized beds (BFB)

Here the gasification agent flow is blown upwards through the distributor, and it passes through a bed of inert material, such as silica and olivine, located at the bottom of the gasifier, where the waste is (Arena and Mastellone, 2005). This fluidized state produce a strong contact between gas and solid with an intense mixing that allow high heat and mass transfer. The feedstock of waste is usually over the bed, along the side walls, and it is fast heated and reacts. The produced gas leaves from the top of the reactor through the free zone between the top of the bed and the top of the reactor (Arena, 2011).

1.3.2.2. Circulating fluidized beds (CFB)

In CFBs the superficial gas velocity increases more than terminal velocity of the solids (more than 3 m/s while in BFBs this velocity is about 1 m/s), therefore there is not a distinct upper surface of the bed and a lot of particles are carried out along with gas out of the bed, this is why a cyclone at the top of the bed is needed, as it cleans the gas collecting the particles and returns them to the bed. Waste is usually fed from the side, and it is fast heated and reacts (Arena, 2011).

1.3.3. Rotatory kiln gasifiers

These kinds of reactors are used in several applications, such as gasification, incineration, cement production, etc. The waste is moved inside a cylinder, slightly inclinated, along with the gasification agent, in order to achieve a good mixing and moving solids into and out a high-temperature reaction zone. The gasification agent is usually at the 'bottom end' of the cylinder. Retention times are higher than in fluidized bed reactors but shorter than in updraft reactors (Christensen et al., 2011; Arena, 2011).

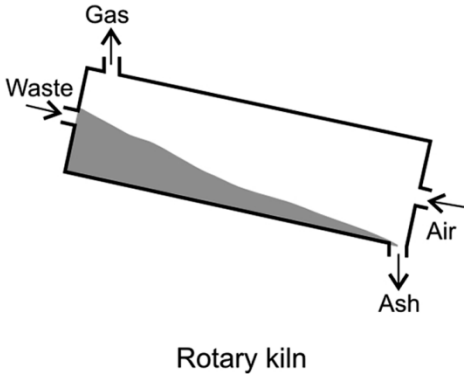

Figure 14. Schematic overview of fluidized bed reactor (Christensen et al., 2011).

These kinds of gasifiers have a high waste volume reduction ratio, which can reach approximately 1/200 of the original waste volume (JAEE, 2011).

1.3.4. Entrained flow gasifiers

Entrained flow gasifiers operate at high pressure, approximately 25 bar, and are usually used to treat coal, residues and mixed plastic waste, because solid fuel is made to feed the gasifier. At first, small particles of fuel are mixed with water to produce the slurry, which is fed into the gasifier with pressurized oxygen. Some fuel is burned in order to achieve high temperatures inside the reactor, so there is a fast conversion of waste into high quality gas (more H_2 and CO content) (Arena, 2011).

1.3.5. Plasma gasifiers

In these reactors, a moving bed gasifier fed with untreated waste, a plasma torche is located in the bottom of the gasifier, so with electricity it generates plasma that comes into contact with the waste, which is converted into a high quality gas, and inorganic matter is vitrified into inert slag. It usually operates at atmospheric pressure and temperatures around 1500-5000 ºC (Arena, 2011).

The main benefit of plasma gasifiers is the high quality of the gas and the high reduction of tar, but it is necessary a huge amount of electricity to work.

1.4. Tar

Tar contain generally hydrocarbon mixtures, which inside of the reactor with high temperature are in a gaseous phase, but they can get cooled to ambient temperature becoming a liquid phase, which can be highly viscose. The main elements which compose tar are carbon and hydrogen, but other elements such as oxygen, nitrogen and sulfur are also found. The major part of tar composition is usually aromatic hydrocarbons (Unger et al., 2002).

Firstly, tar is classified into three different groups: primary, secondary and tertiary. In Table 9, those three groups are described.

Group	Description	Composition
Primary tar	Tar from the pyrolysis output. Temperatures of formation around 200 ºC and 500ºC.	Oxygen rich part contains alcohols, ketons, aldehydes or carbon acids. Oxygen poor part contains bi- and trifunctional monoaromatics, such as phenol, dimethylphenol and cresol.
Secondary tar	Are produced in presence of a gasification agent (oxygen, air or steam). Primary tars react to small gaseous molecules.	Alkylated mono- and diaromatics including heteroaromatics, such as pyridine, furan, dioxin and thiophene.
Tertiary tar	Temperatures of formation over 800ºC.	Benzene, naphthalene, phenanthrene, pyrene and benzopyrene (polynuclear aromatic hydrocarbons PAH).

Table 9. Description and composition of primary, secondary and tertiary tar (Aigner et al., 2009).

Table 10 shows the evolution of tar main component with the temperature.

400ºC	500ºC	600ºC	700ºC	800ºC	900ºC
Mixed Oxygenates	Phenolic Ethers	Alkyl Phenolics	Heterocyclic Ethers	PAH	Larger PAH

Table 10. Transition of tar dependent on temperature (Milne et al., 1998).

Tar can also be classified depending on the molecular weight of the former components. In Table 11 there are explained the different groups of components which form tar depending on the molecular weight.

Tar group	Description	Components
GC-undetectable	Heavy tars	-
Heterocyclic aromatics	It contains hetero atoms, highly water soluble compounds	Pyridine; phenol; cresols; quinoline; isoquinoline; dibenzophenol
Light aromatic (1 ring)	Light hydrocarbons with single ring. No problem with condensability and solubility	Toluene; ethylbenzene; xylenes; styrene
Light PAH compounds (2-3 rings)	Condensation at low temperature, even at low concentration	Indene; naphthalene; methylnaphthalene; biphenyl; acenaphthalene; fluorene; phenanthrene; anthracene
Heavy PAH compounds (4-7 rings)	Condensation at high-temperature at low concentration	Fluoranthene; pyrene; chrysene; perylene; coronene

Table 11. Classification of tars based on the molecular weight (Li et al., 2009).

Tar composition also varies from pyrolysis to gasification outputs, as in pyrolysis tar output the main component with about 70% of concentration are phenols (a primary tar), while in gasification tar output the main components are naphthalenes with a 40% of concentration. The difference between them can be seen in Figure 15 and Figure 16, which are a schematic representation of the composition of tar from pyrolysis and gasification.

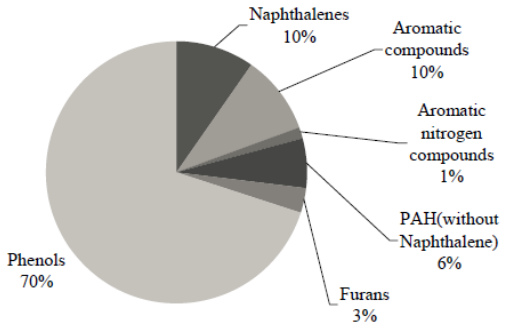

Figure 15. Average tar composition in pyrolysis producer gas (Wolfesberger, 2009).

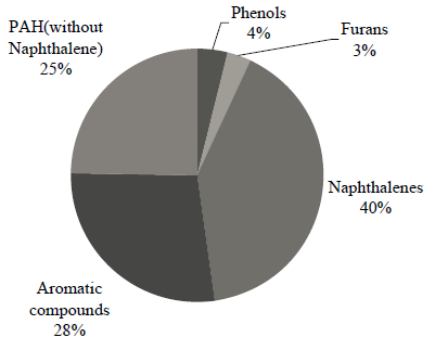

Figure 16. Average tar composition in steam gasification producer gas (Wolfesberger et al., 2009).

Tar content is an important factor in producer gas quality in gasification process, and is essential for pyrolysis process. Tar is undesirable as it presents several problems related to condensation, formation of tar aerosols and formation of more complex hydrocarbons which damage pyrolysis and gasification equipment as well as engines and turbines that run using fuel gas (Salem, 2009). Moreover, tar from pyrolysis output can be used for a second pyrolysis or gasification reactor with a catalyst in order to reduce the overall tar production and get more H_2 and CO from the initial input in the pyrolysis reactor. Therefore, an accurate research of tar content is needed, at different conditions, in order to improve the pyrolysis and gasification process.

1.5. Catalyst

As has been said in the last chapter, it is possible to take more profit from pyrolysis condensable gases output, circulating gases output still at high temperature (it will be a mix of condensable gases and non-condensable gases) through a second pyrolysis or gasification reactor (during the experiments set in the laboratory a second pyrolysis reactor has been used), where with a catalyst it is able to reduce tar content and produce more profitable H_2 and CO content in the output gases. The election of the catalyst is important, as depending on it the tar reduction efficiency will be higher or lower, and there will be more or less problems of clogging, slagging, etc.

There are several kind of catalyst used for this porpose, like dolomite, olivine, limestone, zinc chloride, calcium oxide, alumina, nickel-based catalysts, etc. (Karatas et al., 2012; González et al., 2011). The studied catalysts for this research have been: calcined dolomite, nickel on alumina (Ni on Al_2O_3) and AFRC.

1.5.1. Dolomite and calcined dolomite

Dolomite is a carbonate mineral which is composed of calcium, magnesium and carbonate. Its chemical formula is $CaMg(CO_3)_2$ (Mineral Data Publishing, 2001-2005).

Figure 17. Picture of dolomite from Navarre (Spain).

The use of dolomite as catalyst for two-step pyrolysis favors the heavy hydrocarbon cracking and increase hydrogen production (Simell et al., 1997; Pérez et al., 1997; He et al., 2009). The catalyst causes an increase of steam reforming and water gas shift reactions, therefore tar, H_2S and NH_3 contents decrease, as well as the lower heating value (LHV) of the gaseous outputs (Karatas et al., 2012).

Compared to other natural catalysts, such as olivine and limestone, dolomite is superior as it is more porous, it has higher internal surface area, more sulfur retention, lower cost and more availability. On the other hand, dolomite is less resistant to attrition, more fragile and has less mechanical strength (Corella et al., 1991).

However, CH_4 fraction in the products can decrease using dolomite as catalyst, maybe because of a decrease in hydrogasification and methanation reactions (Corella et al., 1991). Moreover, the use of dolomite produces carryover of fines, attrition and elutrition. Therefore, the level of dolomite used must be controlled.

In order to solve some of the drawbacks of dolomite, one measure often taken is to calcine dolomite, as it gets more effective in the retention of H_2S. The reason why may be the presence of CaO and MgO while dolomite contains $CaCO_3$ and $MgCO_3$ (Karatas et al., 2012).

1.5.2. Nickel on alumina (Ni/Al_2O_3)

Nickel on alumina (Ni/Al_2O_3) is a nickel-based catalyst commonly used as catalyst in pyrolysis or gasification for tar removal.

Figure 18. Picture of KUB-3 (Ni and NiO on Al_2O_3).

This catalyst is very effective for tar removal and producing high quality gas (Aznar et al., 1998; Wang et al., 1998; Bangala et al., 1998). Nickel on alumina is able to produce a methane-rich gas, increasing the heating value of the gaseous products, at the same time that it removes tar (Baker et al., 1996). However, it is easy to deactivate due to

carbon deposition and nickel particle grow, producing a decrease in the active surface area of the catalyst particles. Nevertheless, in order to reduce cocking, a bed of dolomite can be introduced into the reactor (Aznar et al., 1998). This catalyst is widely used because of its commercial availability, effectiveness (in some experiments conversions have reached even 90-92% of the volatile fraction) and relatively cheapness (no more than dolomite) (Li et al., 1996).

The catalyst can be prepared by two different methods. For low concentrations of nickel the method used is usually wet impregnation, while for higher nickel concentrations co-precipitation is used.

1.5.3. AFRC

AFRC is another natural catalyst, such as dolomite, olivine, limestone, etc. It consists on an agglomeration of several kinds of minerals, some of them used as a catalyst for their own, like dolomite. AFRC is the catalyst used for the second pyrolysis reactor which the thesis is studying. The exact composition of AFRC is described in Table 12.

Mineraly	Smectite	Serpentine	Chlorite	Goethite	Quartz	Dolomite		
weight %	70	6	4	2	3	15		
Components	SiO_2	MgO	Fe_2O_3	CaO	Al_2O_3	CO_2	H_2O	Other
weight %	40.4	23.2	7.1	4	3.8	7.1	12.8	1.6

Table 12. Composition of AFRC catalyst.

2. Description of work

2.1. Thermal characterization of MSW equipment

Thermal characterization of MSW has been done by means of thermogravimetry (TG), bomb calorimeter and elemental analysis (EA). It is a reproducible, informative, rapid and relatively cheap method to characterize the quality, composition, kinetics, etc., of organic matter such as MSW, char, tar, etc. Moreover, it is able to work with very small samples of material (Plante et al., 2009).

Thermogravimetric analyzer, bomb calorimeter and elemental analyzer used in order to carry out the characterization of the MSW input and the products of the experiments carried out during this thesis will be explained.

2.1.1. Thermogravimetric analyzer (TGA)

Thermogravimetry (TG) is an analytical technique used to determine the different material's fractions (moisture, volatile fraction, fixed carbon and ashes) and their stability when it is being heated, by monitoring its weight during the experiment.

The experiment is carried out in an inert atmosphere in argon and nitrogen, while the analyzer records the weight of the sample as a function of increasing temperature. For the final stage of the experiment, when combustion of fixed carbon occur, oxygen is introduced in order to oxidation succeed. Inside the analyzer, besides the main crucible with the sample, there is another empty reference crucible, so the analyzer also records the heat flow difference between the two crucibles. This technique is called differential scanning calorimetry (DSC). Therefore, the energy released or absorbed via chemical reactions during heating process is monitored. The thermogravimetric analyzer used for the thesis experiments is a vertical TGA, so the crucible is considered free from buoyancy effects, but it is necessary to calibrate the crucible before starting the experiment to compensate the differential thermal expansion of balance arms (Öner, 2007).

Figure 19 is an example of a graph obtained after the analyzer software on the computer has analyzed the data and has generated the graph representing the evolution of the weight with the increase of the temperature.

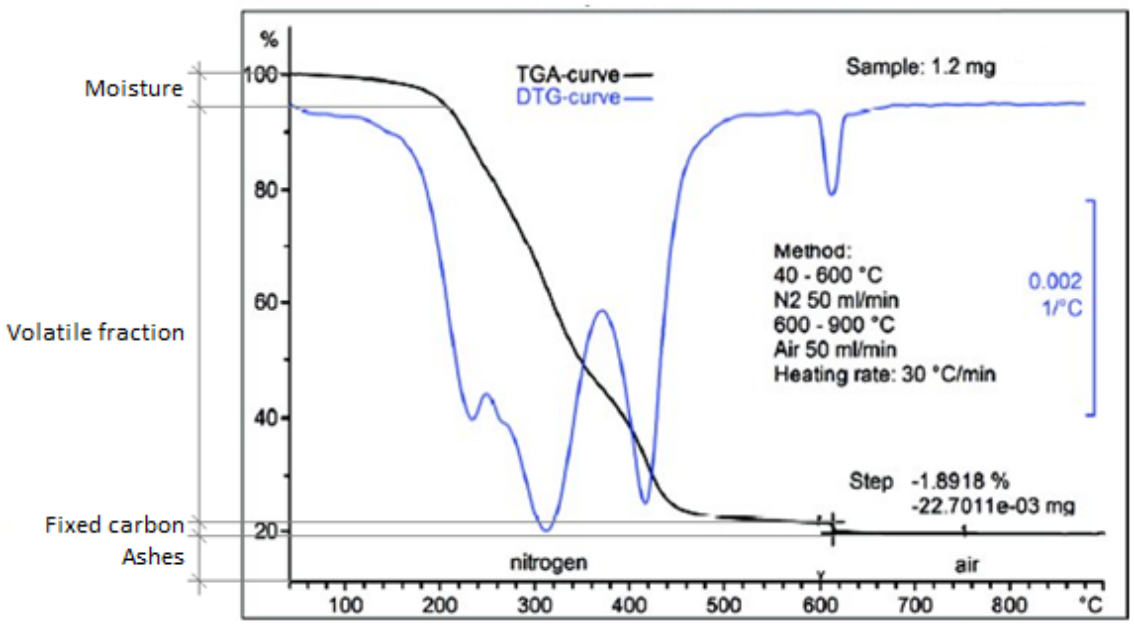

Figure 19. Example graph obtained by TG with the different sections identified (Wagner and Zemo, 2013).

In Figure 19 it can be seen the different stages. In the first stage, quite linear, the moisture is evaporated. The second stage is where volatile fractions are emitted. In the third stage O_2 starts to enter inside the TGA and there is a fast combustion which releases gases (mostly CO_2). Finally in the fourth stage there are only the remaining ashes of the combustion.

The experiment is divided in 4 steps: in the first step the sample is prepared and calibrated, writing down the mass of the empty crucible and the crucible filled with the sample (it will be needed after to calibrate the analyzer); a second step is needed to purge the chamber inside the analyzer where the crucibles are (with argon and nitrogen) during 45 minutes approximately; the third step is when the experiment is carried out

and it ends depending on the heating rate choose (5ºC/min, 10ºC/min or 20ºC/min); and the final step is for cooling the analyzer, in order it can be ready for a new experiment starts.

In this case, all the experiments have been carried out with a heating rate of 5ºC/min, 10ºC/min and 20ºC/min (all but the char outputs, only made with 20ºC/min heating rate, and the RDF and PPD input samples, only made with 10ºC/min heating rate), until the temperature reaches 800ºC in an inert atmosphere (argon), then 20 minutes of isothermal regime with argon and after 20 minutes more of isothermal combustion with O_2.

The reason why with the MSW input samples the experiment has been done with each heating rate is because it is necessary in order to figure out the kinetics of the material.

The thermogravimetric analyzer used to carry out the experiments in this thesis is the simultaneous thermal analyzer NETZSCH STA 409 PC Luxx. Figure 20 is a schematic picture of the thermogravimetric analyzer used.

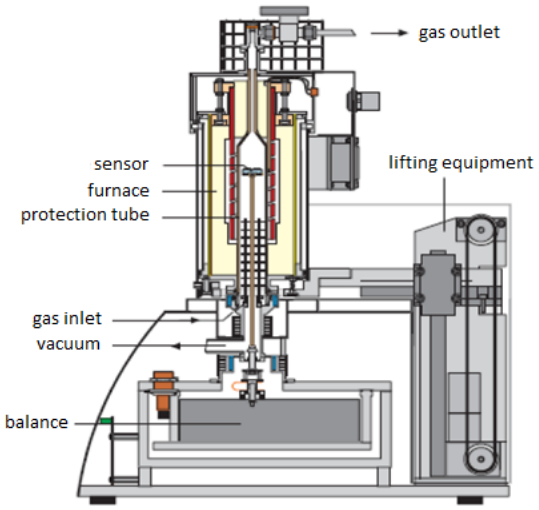

Figure 20. Thermogravimetric analyzer (simultaneous thermal analyzer NETZSCH STA 409 PC Luxx).

The technical information is given in Table 13.

Design	Top-loading systém
Heating	SiC (1500˚C)
Working temperature	20-1550˚C
Heating rate, cooling	0-50 $K.min^{-1}$
Holder	TG-DSC, TG, DTA
Measuring range of the instrument	18 g
Weight of sample	to 18 g
Accuracy of the instrument	2 µg
Atmosphere	Inert, oxidative
Possibility vacuum	to 10^{-2} Pa
Crucibles for TG-DSC	Al_2O_3, Pt-Rh (35 µl)

Table 13. Technical information of Thermogravimetric analyzer (simultaneous thermal analyzer NETZSCH STA 409 PC Luxx).

2.1.2. Bomb calorimeter

The main objective of a bomb calorimeter is to determine the combustion heat (or enthalpy of combustion, ΔH_c^0). Combustion heat means the heat released when all carbon and hydrogen from hydrocarbons is combusted with oxygen to form carbon dioxide and water (Hope College, 2000). Reaction can be seen in Equation 1.

$$C_X H_Y O_Z(s) + \left(X + \frac{Y}{4} - \frac{Z}{2}\right) O_2(g) \rightarrow X CO_2(g) + Y H_2O(l)$$

Equation 1. Combustion of hydrocarbons reaction (Hope College, 2000).

The heat released by the oxidation of other components of the sample, such as sulfur, are also included in the combustion heat.

In a bomb calorimeter the combustion heat is determined by a substitution procedure, comparing the heat released by the sample with the heat obtained from a standardized material with a known calorific value. The sample is burned inside a vessel (also called bomb) in a high-pressure oxygen atmosphere, and after the heat released is absorbed by an absorbing medium, the temperature change of this medium is analyzed. Then, this change in temperature is multiplied by a relation previously found with the energy released or heat capacity of a standardized material. Finally, some correction must been done before obtaining the final results, as is necessary to adjust the values to the heat transfer in calorimeter (Parr, 2007).

Combustion heat is usually exothermic, therefore the value is usually negative (this is why combustion heat is often referred to $-\Delta H_c^0$).

Figure 21 shows a schematic representation of a bomb calorimeter.

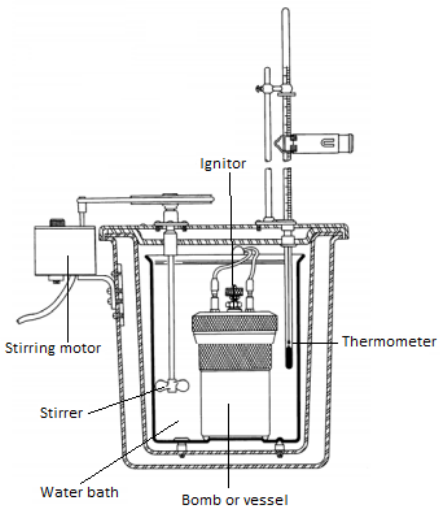

Figure 21. Scheme of a bomb calorimeter (Parr, 2007).

The main parts of the bomb calorimeter are: the bomb or vessel where the combustion of the sample occurs; the water bath which surrounds the vessel agitated by a stirrer; the insulating jacket in order to cancel thermic perturbations from outside the calorimeter;

and the thermometer which measures the temperature changes inside the bucket (Parr, 2007).

Calorimeter used to carry out the experiments in this thesis is an FTT isoperibolic bomb calorimeter from Fire Testing Technology Company Limited. The technical information is given in Table 14.

Type	Isoperibolic
Water temperature	25˚C
Temperature measurement	Resolution 0,001 ˚C
Operating pressure of oxygen (max)	Prescribed in 30 bar, tested 200 bar
Reproducibility [% RSD]	By EN ISO 1716 0,2 %
Operating temperature (max)	30 ˚C
Permissible ambient temperature	< 30 ˚C
Permissible relative humidity	< 55 %
Standardization	Benzoic acid
Tools	steel crucible, ignition wire, cotton
Landfills samples	to 1 g

Table 14. Technical information of calorimeter (FTT isoperibolic bomb calorimeter from Fire Testing Technology Company Limited).

2.1.3. Elemental analyzer (EA)

In order to get a reliable identification and verification of the element composition of the MSW, it is necessary to carry out experiments of organic elemental analysis.

Elemental analyzer is mainly used to determine MSW composition of carbon, hydrogen, nitrogen and sulfur. Inside the elemental analyzer, organic substance undergoes an oxidative decomposition, combustion at high temperature in an oxygen atmosphere, and therefore a reduction of nitrogen and sulfur oxides, followed by thermal conductivity detection (Fadeeva et al., 2007). However, the oxygen content of the sample must be measured separately using pyrolysis (to measure it there must be absence of oxygen in the atmosphere of the sample) and reduction of the sample (Allison et al., 2007). As happens with the oxygen content, inorganic elements must been also analyzed separately. If they are not, they would make average with other species and the results would not be valid. This process produces the formation of carbon dioxide, water, nitrogen and sulfur dioxide.

The analyzer is based on the ion signals intensities from the fragments, which are proportional to the mass concentration of the original species, and the analyzer is able to record them obtaining data (Allison et al., 2007).

Inside the analyzer there is a combustion furnace where the sample inside a crucible is placed. The software used is able to measure the products of combustion during time, so it can finally figure out the fraction of carbon, hydrogen, sulfur and nitrogen originally present in the sample. When the combustion is over the crucible is removed from the furnace.

Elemental analyzer used to carry out the experiments in this thesis is an elemental analyzer Vario Macro Cube from ELEMENTAR. The technical information is given in Table 15.

Gas requirements	helium, oxygen
Helium	
Gas purity	≥ 99,996 %
Pressure in the intake	to 2,5 bar
Gas flow	600 ml/min
Oxygen	
Gas purity	≥ 99,995 %
Pressure in the intake	to 2,5 bar
Gas flow	600 ml/min
Temperature module for CHNS	
Combustion tube	1150 ˚C
Reducing tube	850 ˚C
Landfills samples	to 1,5 g

Table 15. Technical information of elemental analyzer Vario Macro Cube from ELEMENTAR.

2.2. Micro GC (Gas Chromatograph)

A gas chromatograph – mass spectrometer (GC-MS) can measure the content of H_2, CO, CH_4, N_2, CO_2, etc. of a gas flow. GC creates a time separation between measures by mixing in a tube the gas analyzed with a gas (in this case helium) which causes a separation of the components in time. The result of the analysis is shown in a chromatogram, where each peak represents one component of the original mixture. The time when the peak appears indicate which component it is, and the area of the peak measure the amount of the gas in the mixture.

In Figure 22 an example of GC chromatogram is shown.

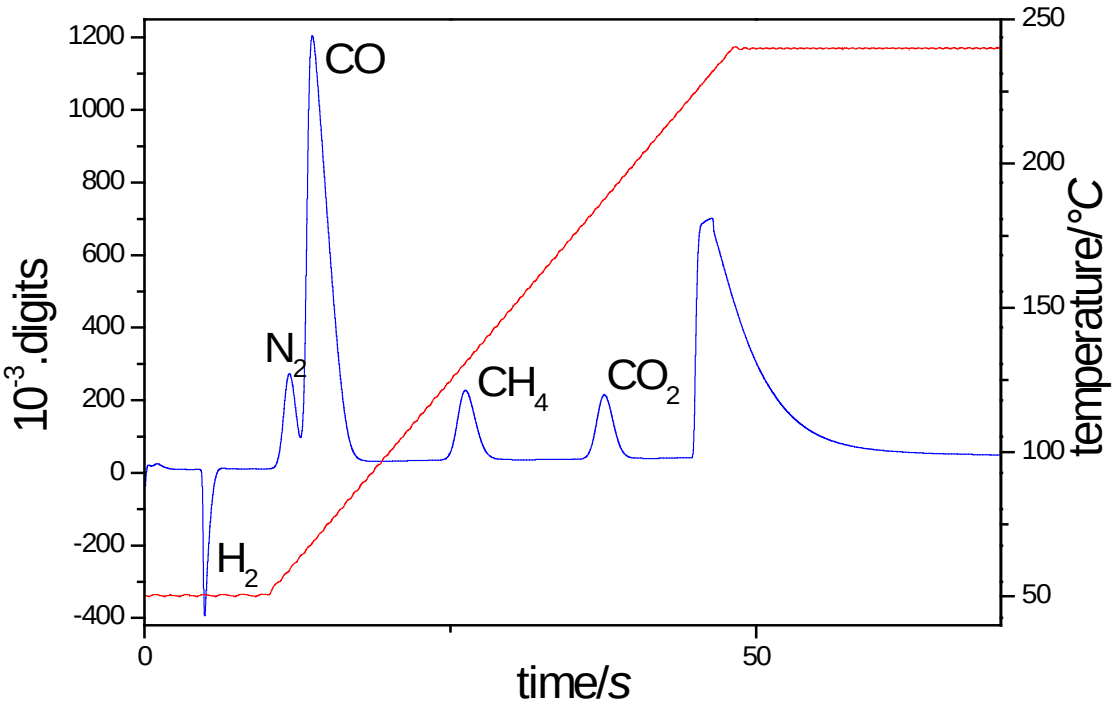

Figure 22. Chromatogram obtained from pyrolysis gases outputs. H_2, N_2, CO, CH_4 and CO_2 are the yields GC can detect.

In Figure 22 it can be seen how depending on the time when a peak appears indicates a different yield, due to different elution times for each one. The area contained between the peak and the base in the horizontal line is used (by means of calibration equations) to find out the molar fraction of every yield.

The GC used in the laboratory is Micro Box III (SLS MICRO TECHNOLOGY, Hamburg, Germany) gas chromatograph with a thermal conductivity detector TCD. The column inside the chromatograph (in which the time separation occurs) is a 65 cm long carbosphere packed column with a 1 cm^2 footprint. It is able to detect components like H_2, CO, CH_4, N_2, CO_2, CH_x and others. The starting temperature is 50ºC with a 5ºC step change until the end temperature of 240ºC.

2.3. Laboratory pyrolysis apparatus

The apparatus employed in the pyrolysis process, consists of a pyrolysis tubular reactor set in series with another fix bed tubular reactor for a catalytic pyrolysis. Both reactors can be heated separately at different temperatures, although during the experiments both were heated at the same temperature by means of tube furnaces. The first reactor is fed with tire sample of MSW (with capacity for 20 g of MSW) which is pushed across the reactor by a rotating screw driven by an electrical motor which is possible to vary the rotation speed in order to set the residence time wanted. Moreover, nitrogen is supplied inside the reactor in order to provide a nitrogen atmosphere during pyrolysis. At the end of the reactor products are divided: char falls into a solid products deposit where it is stored while volatile products (permanent gases and condensable hydrocarbons)

circulate directly to the second pyrolysis reactor, with catalyst inside it, in order to undergo further degradation. This second decomposition is produced by high temperatures and the catalyst, while the first decomposition in the first pyrolysis reactor is produced only by the influence of temperature. After catalytic pyrolysis, product gases pass through a set of 6 impingers, 4 of them containing isopropanol and the 2 left empty, in order to condense tar and other condensable gases. This method for cooling condensable hydrocarbons is standardized. The rest of gases are directed to an ice bath as a precautionary measure for GC-MS (gas chromatographer – mass spectrometer), in order to cool the few possible condensable gases left before the flow is introduced into GC. After, in regular intervals GC takes a little sample of the gas flow which is analyzed, while the main gas flow is released to the atmosphere. Because of entire system takes place in presence of nitrogen, it is regulated through a flow-meter.

Figure 23 represents a scheme of the pyrolysis apparatus used in laboratory during the experiments, including the electronic equipment used in order to analyze the products.

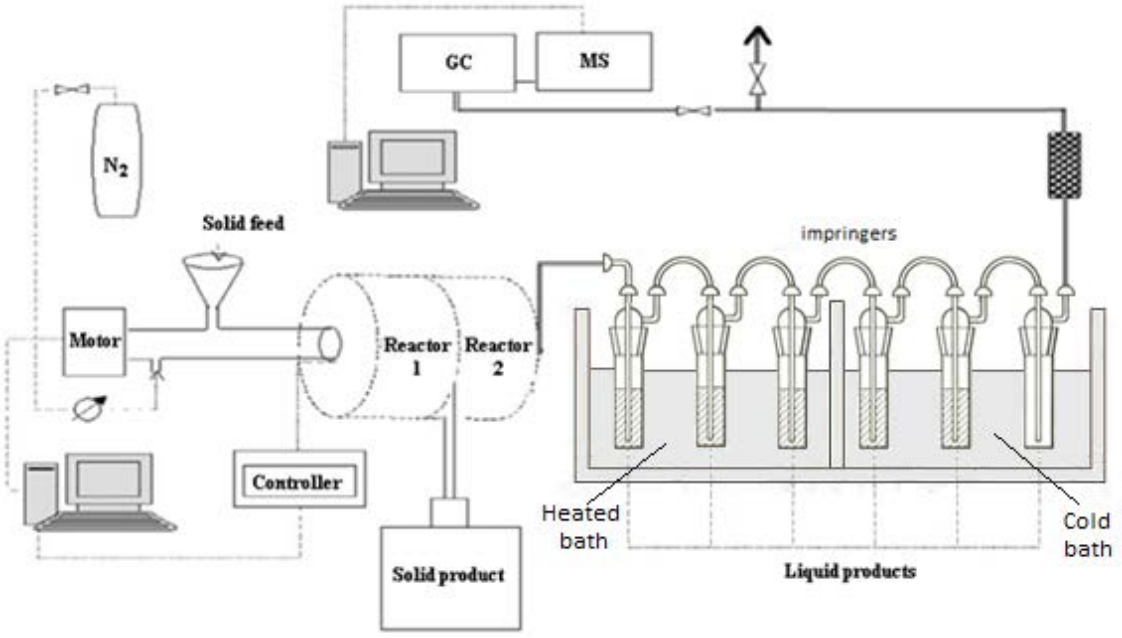

Figure 23. Scheme of the pyrolysis apparatus employed on laboratory.

For further acknowledgement of the tar collection method, the set of impringers is constructed according to the "European Tar Protocol" (Neeft, 2005). Like it can be seen in Figure 22, it consists of six impingers, five of them are filled with isopropanol (IPA) and one is empty. Impingers 1, 2 and 4 are inside a heated bath with a temperature of +35ºC, while impingers 3, 5 and 6 (6 is referred to the empty impinger) are inside a cold bath with a temperature of -20ºC. Therefore, following the order for impingers 1, 2, 3, 4, 5 and 6, the sequence of temperatures for each one is hot, hot, cold, hot, cold and cold. Impingers 2, 3 and 5 have glass-sinters so better gas dispersion will be obtained. The empty impinger is used as a droplet collector. All the set of impingers are placed in a styrox box which has a styro-foam wall to isolate warm from cold baths. When the tar (and other condensable gases) collection ends, the content inside impingers is collected

in order to analyze it, while tubing and glass parts are washed with isopropanol solution (Romar et al., 2010).

Finally, for more detail of the first pyrolysis tubular reactor employed, Figure 24 shows the inside of this rector were the screw rotate in order to push down the sample through the reactor.

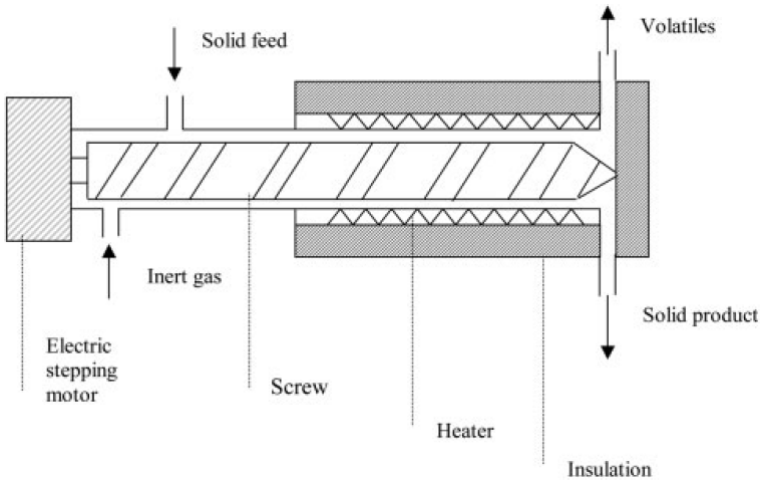

Figure 24. Scheme of the first pyrolysis reactor with the rotating screw inside.

3. Results and discussion

3.1. Thermal characterization of MSW results.

Previous to the pyrolysis experimentation, experiments with thermogravimetry analyzer, calorimeter and elemental analyzer have been carried out in order to characterize the MSW samples used. With these experiments, the exact composition of the different materials which can be found in a MSW sample has been found.

With data obtained, it has been possible to complete an elemental analysis and a proximate analysis, followed by the determination of the combustion heat of each material former of MSW.

3.1.1. Elemental analysis and proximate analysis results

First, a sample of MSW is divided into the different materials which compose it: polystyrene (PS), polyurethane (PU), textile, white paper, recycled paper, low density polyethylene (LDPE) and high density polyethylene (HDPE). With elemental analyzer the content of nitrogen (N), carbon (C), hydrogen (H) and sulfur (S) of each one is found, after calculating the average value of different experiments done with the same component. Then, with TG the approximate analysis of each component is carried out, also finding the average value between three experiments carried out with the same material but at different heating rate (5ºC/min, 10ºC/min and 20ºC/min). The results

found are the moisture content, the volatile fraction, the fixed carbon content and the remaining ashes of each material. So, with the weight percentage of N, C, H, S and ashes found, the rest is the oxygen contained in the sample, so the elemental analysis is completed.

An example of the TG curves obtained is shown in Figure 25. It is the TG curve of a textile sample carried out with 20ºC/min heating rate. In the Appendix B.1 the rest graphs obtained with the TG curves are shown.

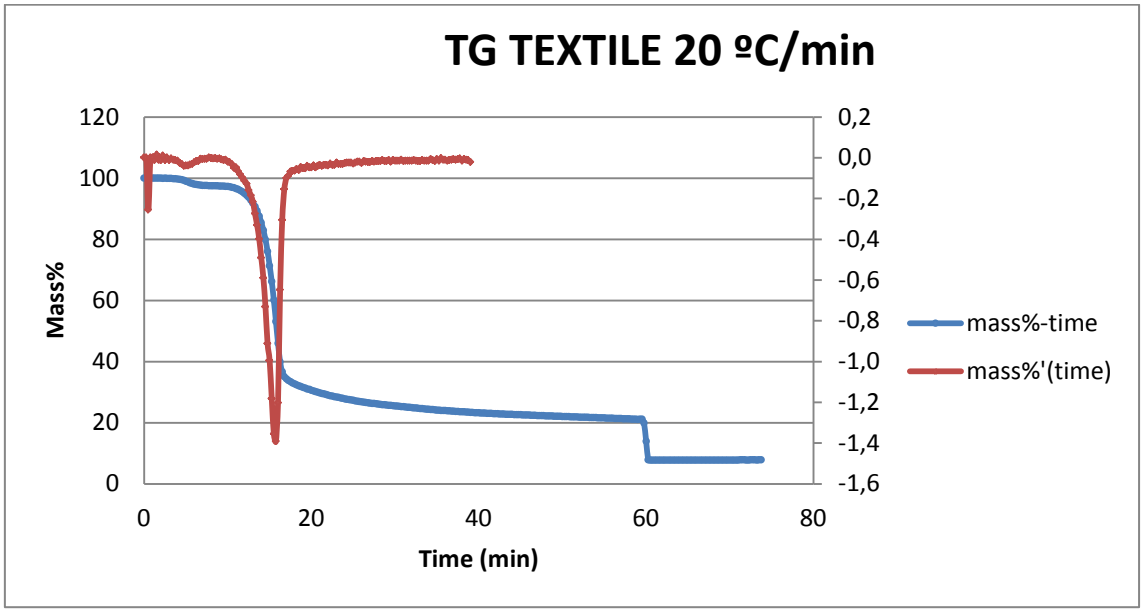

Figure 25. TG curve for a textile sample carried out at 20ºC/min heating rate. The blue line represents the decrease of mass during time, while the red line represents the derivative curve of the mass-time function.

In Figure 25 the different parts of the curve can be easily seen. Initially, the moisture is released, which can be seen in that little step on mass-time curve, which correspond to the first small minimum in the derivative line. The volatile fraction is then the mass released between the point where moisture step ends and where the fixed carbon step starts (the last step found after 60 minutes), which correspond to the big minimum in the derivative curve. Finally, the remaining mass is the ash content. In this TG curve, the results are: 2,47% of moisture, 76,39% of moisture, 13,31% of fixed carbon and 7,82% of ash content.

In Table 16 the first results obtained from the elemental and proximate analysis are given.

								PROXIMATE ANALYSIS		
ELEMENTAL ANALYSIS										
NAME	Weight (mg)	N	C	H	S	O*	ASH	M. (1)	VF (2)	FC (3)
Textile	24,05	4,33	54,36	6,53	0,17	28,96	5,65	3,26	80,89	10,21
PS	21,04	0,65	88,66	7,60	0,06	-0,15	3,19	0,00	96,81	0,00
LDPE	26,50	0,93	79,38	13,63	0,07	2,07	3,93	0,00	96,07	0,00
White Paper	23,94	0,13	45,58	7,00	0,05	30,43	16,81	1,33	78,30	3,56
Recycled Paper	21,74	0,70	41,57	5,92	0,17	41,95	9,69	2,26	77,03	11,03
HDPE	27,21	1,24	82,49	13,06	0,00	1,83	1,38	0,00	98,62	0,00
PU	25,77	4,38	63,59	8,34	0,47	0,50	22,72	0,00	77,28	0,00

Table 16. First results obtained from the elemental and proximate analysis. All contents are given in percentage (%). **(1)** MOISTURE. **(2)** VOLATILE FRACTION. **(3)** FIXED CARBON. *The O fraction has been found by the difference between 100 and the total of N + C + H + S + ASH. Problematic values are in red.

As it can be seen in Table 16, there is an error in the final result of the O content in PS. The reason of this oxygen value in PS is the big amount of ashes found in TG results (3,19%), as for LDPE, HDPE and PS the amount of ash should be 0% and therefore should be 100% of volatile fraction as many studies suggest (İTÜ, 2011; Ryu et al., 2004; Kayacan and Dogan, 2008; Sichina, 2006; Lordi and Bueno, 2012; Almustapha and Andersen, 2011). The reasons of this error can be several: a bad calibration on the TG, because the materials are not pure (maybe are blends of various polymers or a mixture of them), a human error, etc. In order to get better results, a correction has been done, considering a 0% on the O content of PS (as it is almost 0%). The corrected results are shown in Table 17.

								PROXIMATE ANALYSIS		
ELEMENTAL ANALYSIS										
NAME	Weight (mg)	N	C	H	S	O	ASH	M. (1)	VF (2)	FC (3)
Textile	24,05	4,33	54,36	6,53	0,17	28,96	5,65	3,26	80,89	10,21
PS	21,04	0,65	88,66	7,60	0,06	0,00	3,04	0,00	96,96	0,00
LDPE	26,50	0,93	79,38	13,63	0,07	2,07	3,93	0,00	96,07	0,00
White Paper	23,94	0,13	45,58	7,00	0,05	30,43	16,81	1,33	78,30	3,56
Recycled Paper	21,74	0,70	41,57	5,92	0,17	41,95	9,69	2,26	77,03	11,03
HDPE	27,21	1,24	82,49	13,06	0,00	1,83	1,38	0,00	98,62	0,00
PU	25,77	4,38	63,59	8,34	0,47	0,50	22,72	0,00	77,28	0,00

Table 17. Corrected results from the elemental and proximate analysis. All contents are given in percentage (%). **(1)** MOISTURE. **(2)** VOLATILE FRACTION. **(3)** FIXED CARBON. *The O fraction has been found by the difference between 100 and the total of N + C + H + S + ASH. O values changed are in green, while the changed results from TG are in blue.

The O content in PS has been considered 0% and therefore there is a 3,04% of ash content, remaining the same volatile fraction. This is of course an approximation, because the O content in PS should be 0% if it was pure PS, but in reality there is always some impurity.

As in Table 17 can be seen, PS, LDPE and HDPE have the most elevated volatile fraction and less ashes and fixed carbon, with low O content. They are mainly carbon and hydrogen which means that in absence of oxygen will generate more H_2, CH_4, polyolefins (mainly ethylene) and benzene during pyrolysis (CH_4 in greater proportion). PU instead will generate more CO_2 due to it contains oxygen in its molecular structure, which is not desired because of its environmental impact (Kaminsky, 1993; CDS, 2009; CDS, 2014). Paper and textile generate more ashes and fixed carbon caused by their significant content of oxygen and, therefore, less H_2 and CH_4 will be produced. The main products from pyrolysis of paper will be complex hydrocarbons derived from cellulose such as avicel, levoglucosan, acetates, and alkaline salts (Evans et al., 2006). It can be bad for the reactor and the catalyst because of the carbon deposition which can damage the equipment. Moreover, textile and PU have higher content of nitrogen and sulfur (PU has the higher content of sulfur). A big amount of sulfur in the composition can lead to an increase of the H_2S generated, which must be removed by the catalyst in the second reactor in order to obtain a cleaner and higher quality gas, and in order to be respectful to the environment.

3.1.2. Calorimeter results

With calorimeter experiments the combustion heat values have been found for each different material which composes the MSW sample used: polystyrene (PS), polyurethane (PU), textile, white paper, recycled paper, low density polyethylene (LDPE) and high density polyethylene (HDPE). Two experiments with each same material have been carried out in order to be more confident in the data obtained. Therefore, the final combustion heat of each material is the average of both results found in those experiments. Results are found in Table 18 while the original data used is shown in Appendix B.2.

Type of residue	Combustion Heat (MJ/kg)
Textile	20,58
PS	42,09
LDPE	44,04
White Paper	13,99
Recycled Paper	14,58
HDPE	34,70
PU	21,56

Table 18. Combustion heat of the different materials which compose a MSW sample expressed in MJ/kg.

The materials with lower combustion heat are white paper and recycled paper followed by textile. Those materials have a lower combustion heat because their chemical structure is easy to degrade, and because of the high content of oxygen. The materials with higher combustion heat are LDPE and PS because of their stable chemical structure with simple bonds, CH_2 groups and low content of oxygen, while HDPE and PU (PU have also simple bonds of nitrogen which decrease the combustion heat) with a less stable chemical structure have a lower combustion heat (FAA, 2001). Moreover, there is a direct relation between the combustion heat and the volatile fraction, as those materials with higher volatile fraction have a higher combustion heat. This is because of volatile fraction is the fraction which will be combusted, so the higher it is the higher amount of heat it will release when it combust.

The study of the combustion heat of each material is needed as the higher it is for a specific mixture, higher heating value of the output gases can be achieved.

3.2. Kinetics analysis

Thermogravimetric analysis of each MSW component has been carried out at three different heating rates: 5ºC/min, 10ªC/min and 20ºC/min. It allows carrying out kinetics analysis, by means of numeric methods approximation and optimization. The method used to find out activation energy (E) and pre-exponential factor (A) is the isoconversional kinetic analysis. This method is based on evaluating the dependence of the activation energy on temperature (or conversion) in order to predict kinetics and explore the mechanisms of thermally simulated process. Isoconversional method applies the Arrhenius equation to a narrow temperature interval, ΔT. This temperature interval changes along with the conversion extent (α) and therefore it is possible to know the variation of the activation energy throughout all the temperature range of the experiment (Vyazovkin et al., 2006). The main single-step kinetic equation and the isoconversional principal equation (stating that at a constant conversion extent the reaction rate is only function of the temperature) are shown in Equation 2 and Equation 3.

$$\frac{d\alpha}{dt} = A\, exp\left(\frac{-E}{RT}\right) f(\alpha)$$

Equation 2. Single-step kinetic equation.

$$\left[\frac{dln(d\alpha/dt)}{dT^{-1}}\right]_{\alpha} = -\frac{E}{R}$$

Equation 3. Isoconversional principal equation.

By using different heating rates (β) different rates ($\frac{d\alpha}{dt} = \frac{d\alpha}{dT}\beta$) can be determined at the same conversion. In Figure 26 the isoconversional method of approximation based on the Arrhenius equation (which is shown in the same figure) is explained.

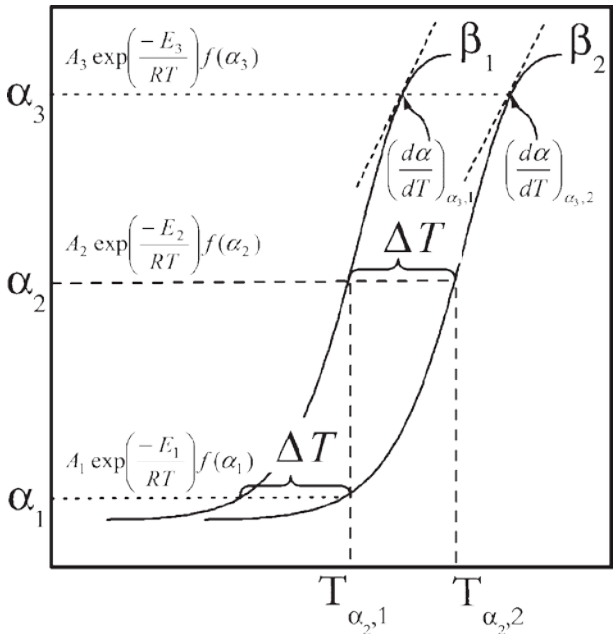

Figure 26. Isoconversional method of convertions for kinetic parameters (Vyazovkin et al., 2006). A: pre-exponential factor. E: Activation energy. R: Gas constant. T: Temperature. ΔT: Temperature interval. α: Conversion extent. β: Heating rate.

The conversion curves obtained from the thermogravimetric data of one MSW component studied in this thesis where the temperature interval changes along with the conversion extent can be seen in Figure 27.

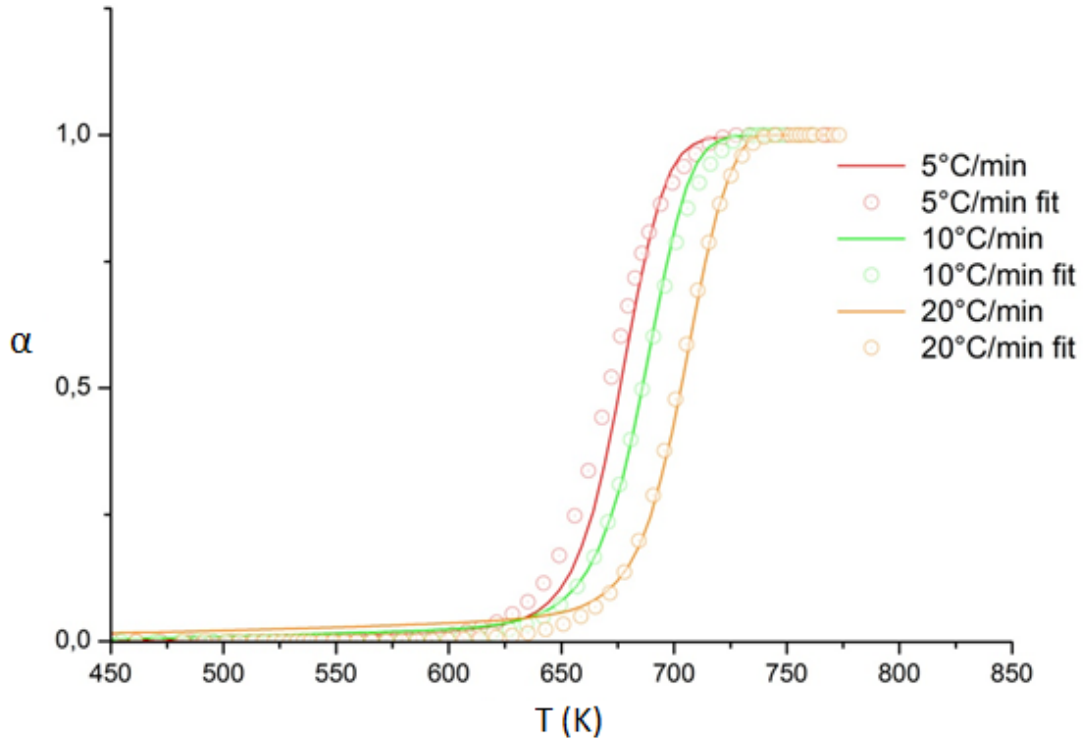

Figure 27. Conversion curves at different heating rates (5ºC/min, 10ºC/min and 20ºC/min). The dotted curves are from the experimental values and the continuous lines are the regression lines of these dotted lines.

In order to check the right conversion of conversion curves, the derivative curve for each one in Figure 27 has been calculated and represented in Figure 28.

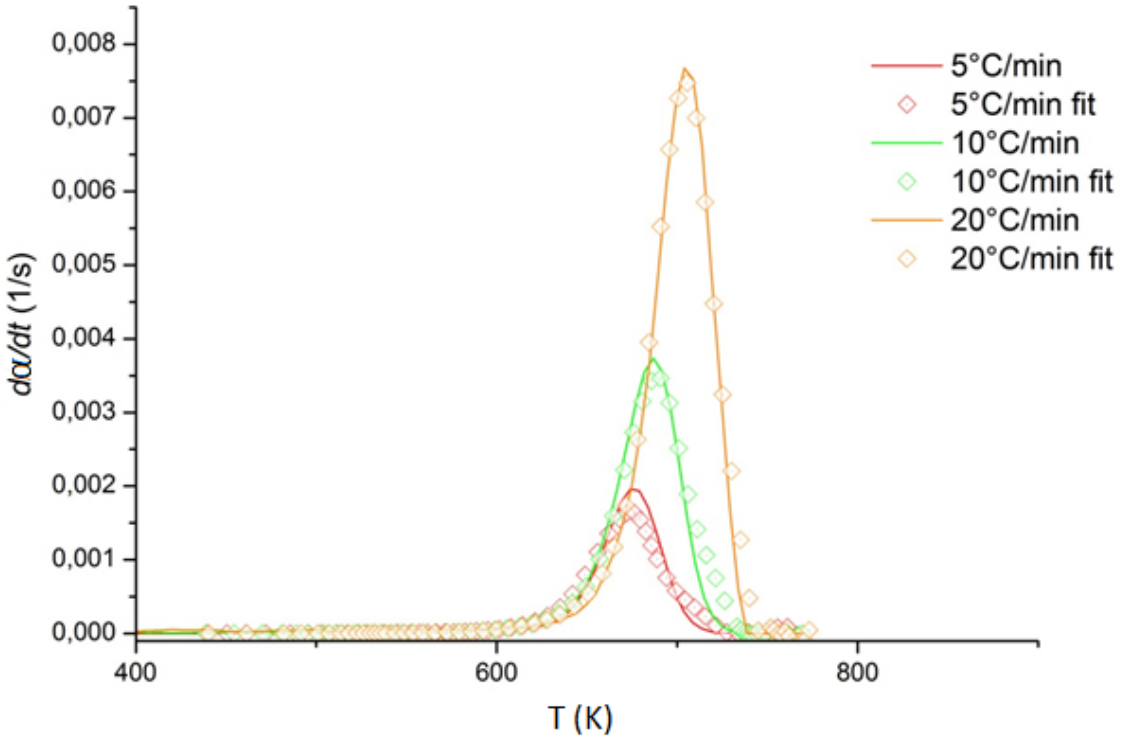

Figure 28. Derivative curves from conversion curves at different heating rates (5ºC/min, 10ºC/min and 20ºC/min). The dotted curves are from the experimental values and the continuous lines are the regression lines of these dotted lines.

As can be seen in Figure 28, the calculated curves match with the experimental points in conversion curves, which indicate a good fit.

After iteration until final conversion the final values of activation energy (E) and pre-exponential factor (A) are found. The final values are shown in Table 19.

	FIRST STEP		SECOND STEP	
SAMPLE	**E (J/mol)**	**A (s^{-1})**	**E (J/mol)**	**A (s^{-1})**
White Paper	200094	$6{,}36 \times 10^{14}$	237358	$2{,}11 \times 10^{11}$
Recycled Paper	240925	$5{,}65 \times 10^{18}$	-	-
HDPE	194386	$1{,}02 \times 10^{12}$	406893	$5{,}33 \times 10^{19}$
LDPE	274784	$1{,}63 \times 10^{17}$	-	-
PS	182902	$5{,}14 \times 10^{11}$	-	-
PU	198269	$7{,}97 \times 10^{13}$	-	-
Textile	220544	$1{,}25 \times 10^{17}$	-	-

Table 19. Activation energy (E) and pre-exponential factor (A) for each MSW component.

These values have been found from calculating an average of the activation energy (E) and pre-exponential factor (A) dependence on the conversion extent curves. These curves are shown in Figure 29 and Figure 30 respectively.

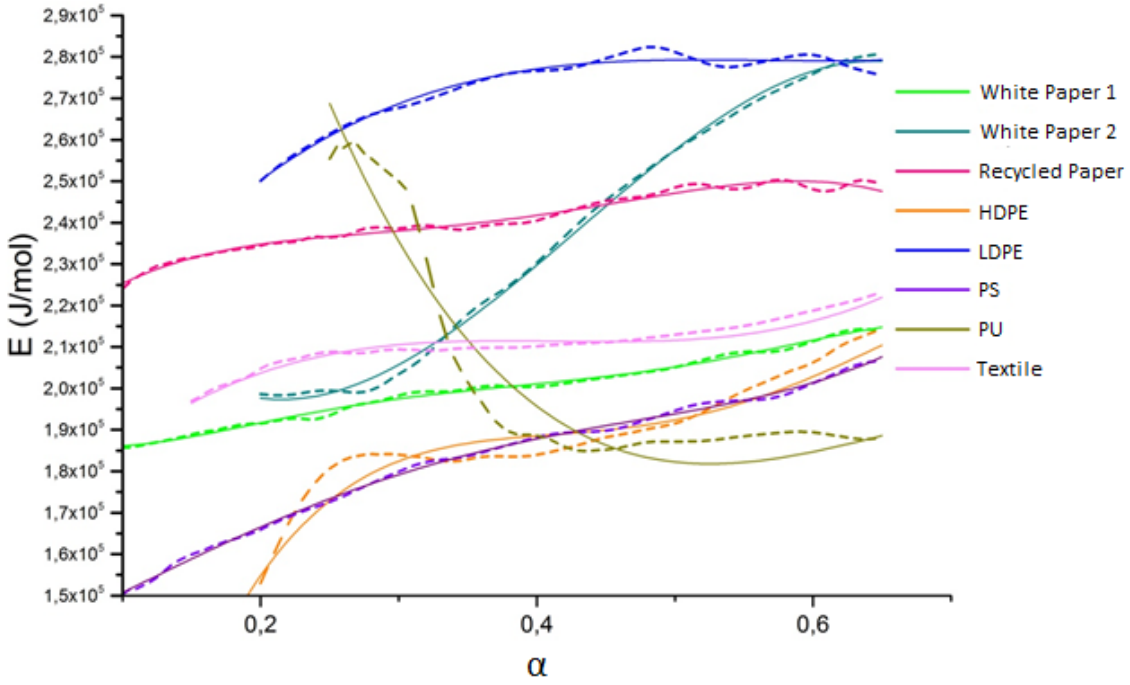

Figure 29. Activation energies (E) dependencies obtained for the thermal degradation of white paper, recycled paper, high density polyethylene (HDPE), low density polyethylene (LDPE), polystyrene (PS), polyurethane (PU) and textile studied in TGA experiments. The dotted curves are from the experimental values and the continuous lines are the regression lines of these dotted lines. E: Activation energy. α: Conversion extent.

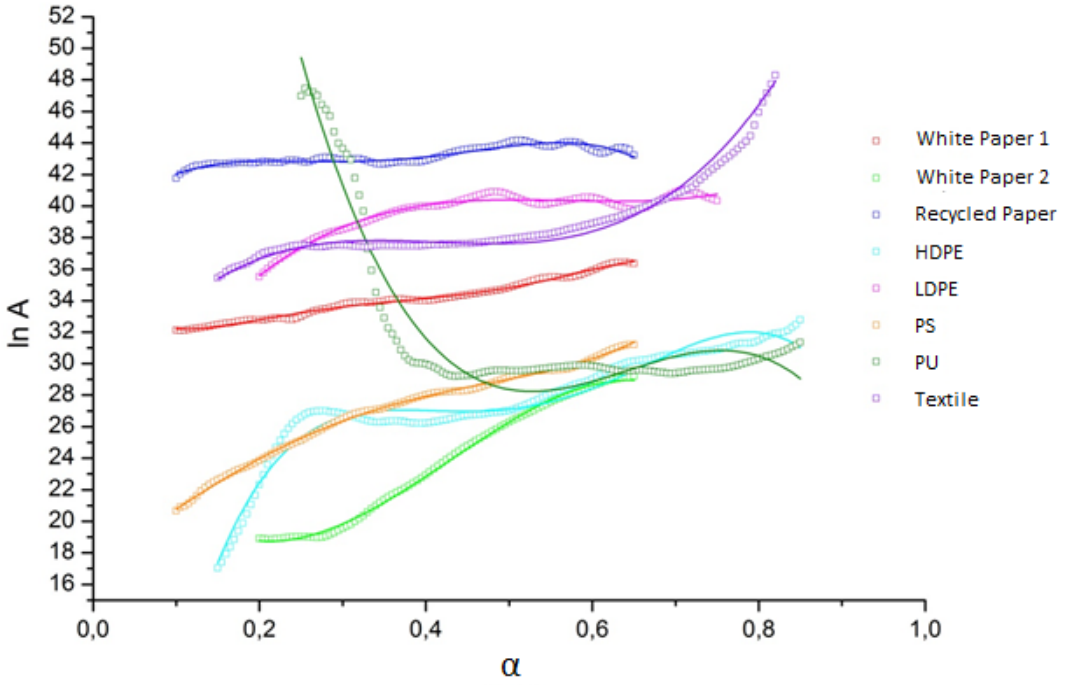

Figure 30. Pre-exponential factors (A) dependencies obtained for the thermal degradation of white paper, recycled paper, high density polyethylene (HDPE), low density polyethylene (LDPE), polystyrene (PS), polyurethane (PU) and textile studied in TGA experiments. The dotted curves are from the experimental values and the continuous lines are the regression lines of these dotted lines. A: Pre-exponential factor. α: Conversion extent.

3.3. Thermal characterization of RDF and PPD results

In order to elaborate a better study of the pyrolysis results, the content of the mixture of MSW introduced into the first reactor has been fixed. Two different mixtures have been considered: RDF and PPD.

RDF (Refuse Derived Fuel) results from sorting (it has a specific content of each component, in this case a specific content of textile, paper, PU, PS, HDPE and LDPE) and drying MSW, and it is focused on producing a high calorific fuel taking from MSW its high calorific fractions (VADEB, 2012). Moreover, it can benefit recycling other lower calorific fractions of MSW which can be more easily recycled (EC, 2003).

PPD stands for the heavy fraction of RDF. It means that it is a mixture similar to RDF, with the same purpose to get the higher calorific fractions of MSW, but in the mixture there is less content of paper and more PE, textile and PU. Moreover, this mixture includes some inorganics.

The composition of RDF and PPD samples can be seen in Table 20.

Samples	RDF (%)	PPD (%)
White paper	63,17	19,37
Recycled paper		
LDPE	15,78	37,30
HDPE	19,10	3,82
Textile	1,94	32,41
Polystyrene	0	0
Polyurethane	0	6,81

Table 20. Composition of RDF and PPD samples. Values are expressed in percentage.

As Table 20 shows, the main differences between those two mixtures are the content of paper, as RDF has significantly more paper content than PPD (white paper and recycled paper are not distinguished because of the difficulty of sorting both kind of paper), the increase in the amount of LDPE and Textile content in PPD while there is a decrease in HDPE, and the presence of PU in PPD while in RDF there is no content of PU.

For TG experiments, several experiments where made with each kind of mixture, in order to have more reliable results. In Table 21 the proximate analysis for RDF and PPD is shown. The TG curves used in order to carry out the proximate analysis are given in Appendix B.3.

MATERIAL	MOISTURE	VOLATILE FRACTION	FIXED CARBON	ASHES
RDF	1,33	77,35	0,000	21,32
PPD	1,15	88,14	3,74	6,97

Table 21. Proximate analysis for RDF and PPD. Values are expressed in percentage. Unusual numbers are painted in red.

Results in Table 21 can be explained largely for the composition of each mixture. The increase of volatile fraction in PPD is caused by the increase of LDPE and PU content in this mixture (while there is only a few decrease in HDPE), which are mainly volatile fraction. The same way can be explained the high content of ashes in RDF, as it has higher amount of paper content which generate this amount of ashes. Finally, there is an unusual result in RDF fixed carbon content, as for RDF composition there should be some content (like fixed carbon content of PPD is 3,74%). This unusual value can be explained by an error of measurement in TG, caused by some remaining oxygen from previous experiments which remains inside the furnace, the nitrogen flow introduced in TG is not able to remove it, and sample undergoes a slow combustion during time at high temperatures that do not let the combustion step occurs.

As PPD release a higher volatile fraction, during pyrolysis process more gases will be released between condensable and non-condensable gases.

After the characterization of RDF and PPD samples, everything is ready to start the pyrolysis experiments, and analyze the results.

3.4. Products results

After all pyrolysis experiments in laboratory have been done, tar and condensable parts from impingers are collected, char from first pyrolysis reactor are collected and analyzed, and non-condensable gases from catalytic pyrolysis reactor are measured and analyzed too. Non-condensable gases have been analyzed by gas chromatography (GC) while for the analysis of char a thermal characterization has been carried out, with thermogravimetric analysis, elemental analysis and calorimetric analysis.

During the performance of the experiments, different temperatures in the reactors have been considered in order to compare the influence of temperature in the process and determine the most favorable conditions. Pyrolysis process has been carried out at 600, 650, 700, 750 and 800ºC. Therefore, GC analyses, elemental analyses, thermogravimetric analyses and calorimetric analyses have been carried out for each temperature. Moreover, char, tar and gases collection and measurements have been also done for each temperature.

3.4.1. Products obtained

The content of char generated after first pyrolysis, tar generated and non-condensable gases released after second reactor have been measured for each temperature and for each different MSW mixture (RDF and PPD). The content percentage of those outputs from the samples inputs is given in Table 22.

SAMPLE	RDF (weight %)			PPD (weight %)		
T (°C)	Char	Tar	Gases	Char	Tar	Gases
600	40,10	0,40	59,50	46,14	0,27	53,59
650	39,00	0,39	60,61	53,22	0,21	46,56
700	36,10	0,33	63,57	43,24	0,19	56,56
750	37,10	0,34	62,56	52,16	0,10	47,74
800	36,80	0,30	62,90	57,75	0,12	42,13

Table 22. Char, tar and non-condensable gases content for each temperature set and for each different MSW mixture (RDF and PPD). Values are expressed in weight percentage.

As it can be seen in Table 22, there is a clear trend to obtain less char, less tar and more gases as the temperature set in the reactors increases. This trend is less clear in PPD results as the char content decreases with temperature with the exception of 650ºC which has higher content than 600ºC and more important 800ºC, which has the most elevated value of char content. Moreover, there is a decrease on the gases production after 700ºC, reaching its lowest value at 800ºC.

Lower temperatures have not been considered as for lower temperatures the composition of products has higher amount of tars. This occur because of at temperatures below 400ºC the reduction of tar is only produced by the condensation reactions at gas/vapor product temperatures, while for higher temperatures than 500ºC severe secondary cracking reactions start producing a higher conversion of the carbon in the waste and a decrease in tar content (Bridgwater et al., 1999). Moreover, tar increases

as a higher heating rate is set and char increases with slow heating rates with relatively low temperatures. To obtain more equal weight content distribution in products, moderate heating rates with moderate final temperatures must be set. For high heating rates up to high temperatures oils undergo further broken down and gas yield increases, whether if after the process a rapid quenching occur (flash pyrolysis) the products obtained can be mainly tars instead of gases. Finally, if the aim of the process is to get high gases fraction, the suitable conditions are slow heating rates up to high final temperatures (Christensen et al., 2011). Shorter residence times and char rapidly removal from the reactor can also increase tar content (Bridgwater et al., 1999).

Figure 31 shows an idealized representation of the evolution of tar, char and gases content while the temperature increases.

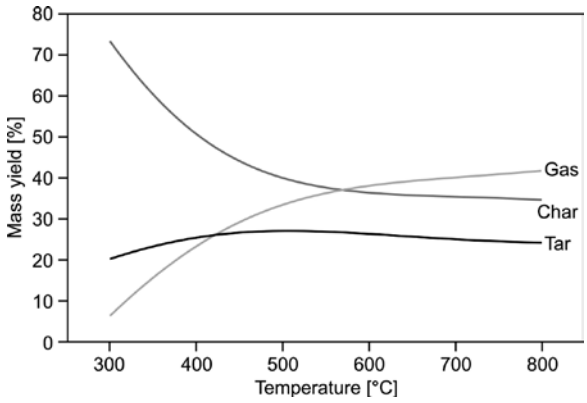

Figure 31. Idealized representation of the relation between tar, char and gases content with temperature. Note that in practical application other factors can induce to a significantly different representation (Christensen et al., 2011).

In contrast with idolized Figure 31, in Figure 32 the representation of the relation between tar, char and gases content and temperature for RDF and PPD is shown.

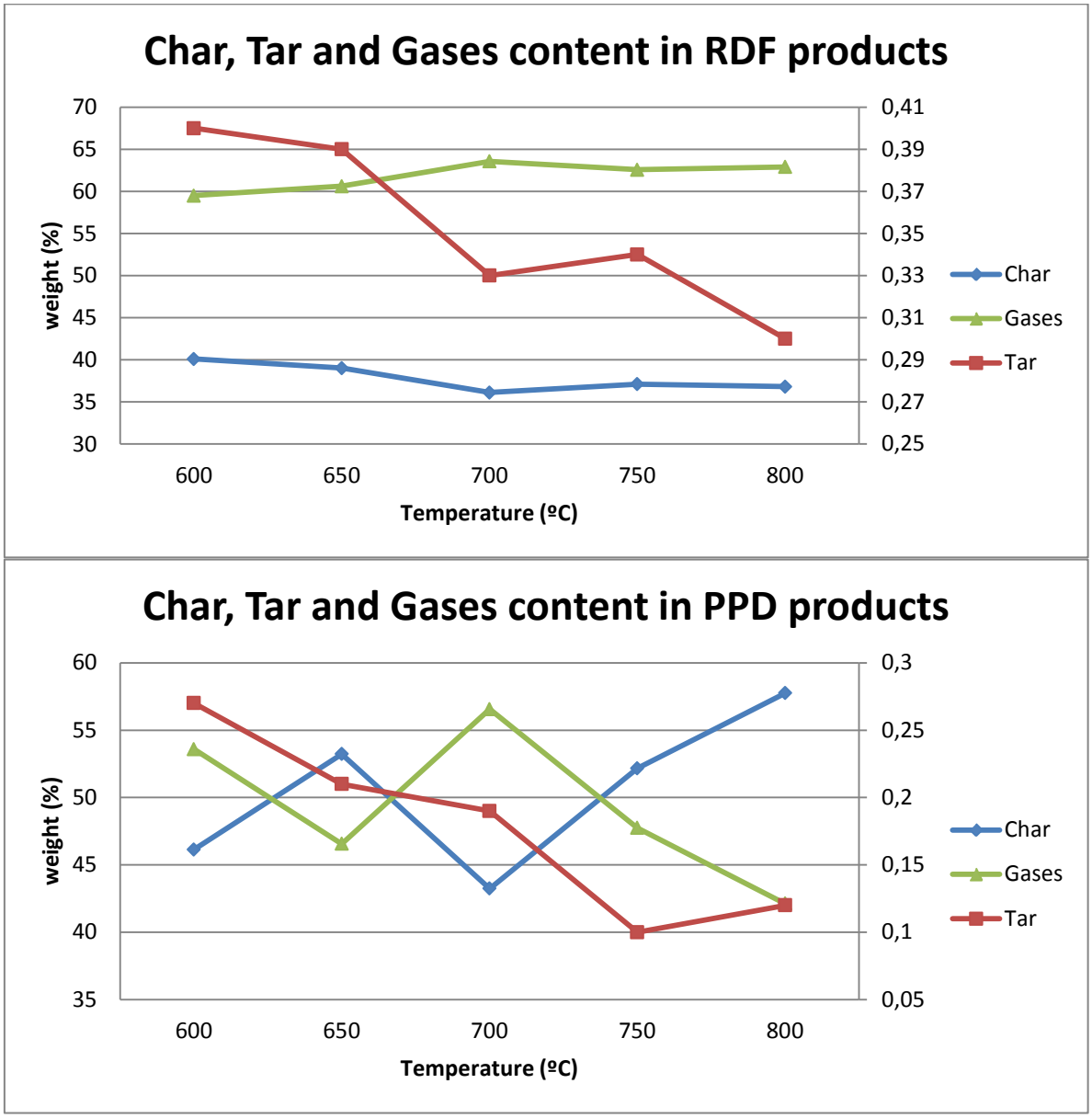

Figure 32. Relation curves between char, tar and gases content and temperature for RDF and PPD.

The reason why for PPD mixture there is not a lineal trend in char decreasing and gases increasing as the temperature increases (it is more similar to a parabolic trend, with an optimum at 700ºC) can be its composition. Like happen with some biomass wastes containing cotton, corn, rice, grass, straw, stover, etc. due to the chemical structure and composition at high temperatures tar are low but solid yield increases which produce a gases content reduction (Amutio et al., 2012). In this case PPD introduces PU, more textile and LDPE and less paper and HDPE, which for its singular chemical composition can lead to the same situation. Therefore, it can be seen that the optimal temperature condition for RDF tar reduction is 800ºC and for PPD 750ºC. However, the optimal temperature condition for gases production and char reduction for RDF and PPD is 700ºC.

Moreover, using RDF mixture for the pyrolysis process less tar and char, and more gases are obtained than using PPD.

3.4.2. Micro GC (gas chromatographer) results

During pyrolysis process measures in GC have been periodically done obtaining different values for the gas content during all process. The data has been collected and analyzed, and after excluding N_2, the maximum values of H_2, CO, CH_4, CO_2 and residual non-condensable gases have been obtained. This residual gases are more complex non-condensable gaseous hydrocarbons with more carbon (C_xH_y), such as C_2H_4 (ethylene), C_2H_6 (ethane), C_3H_6 (propene), etc., and non-metal hydrides like H_2S (Ta-Chuang et al., 2006).

In Table 23 and Table 24, the maximum values of gas contents for RDF and PPD respectively are given.

	MAXIMUM VALUES RDF				
T(°C)	**H_2**	**CO**	**CH_4**	**CO_2**	**Residue**
600	0,26	0,03	0,06	0,06	0,59
650	0,22	0,06	0,13	0,11	0,48
700	0,21	0,08	0,18	0,12	0,41
750	0,23	0,11	0,24	0,11	0,31
800	0,33	0,19	0,14	0,04	0,30

Table 23. Maximum values of H_2, CO, CH_4, CO_2 and residue content from non-condensable gases released of RDF mixture. Values are given in weight fraction (x).

	MAXIMUM VALUES PPD				
T(°C)	**H_2**	**CO**	**CH_4**	**CO_2**	**Residue**
600	0,23	0,08	0,08	0,12	0,49
650	0,25	0,10	0,09	0,15	0,41
700	0,23	0,10	0,10	0,16	0,41
750	0,27	0,14	0,10	0,10	0,39
800	0,29	0,18	0,09	0,09	0,35

Table 24. Maximum values of H_2, CO, CH_4, CO_2 and residue content from non-condensable gases released of PPD mixture. Values are given in weight fraction (x).

In Table 23 and Table 24 it can be seen as at lower temperatures there is a higher production of H_2 and CO, and a lower production of residue for PPD than for RDF. Otherwise, at higher temperatures there is a higher production of H_2 and CO, and a lower production of residue for RDF than for PPD. Overall, CH_4 production is always higher for RDF and CO_2 production is always higher for PPD.

For better appreciation of the values in Table 23 and Table 24 and their evolution with temperature, a graph has been elaborated for RDF and PPD which is represented in Figure 33.

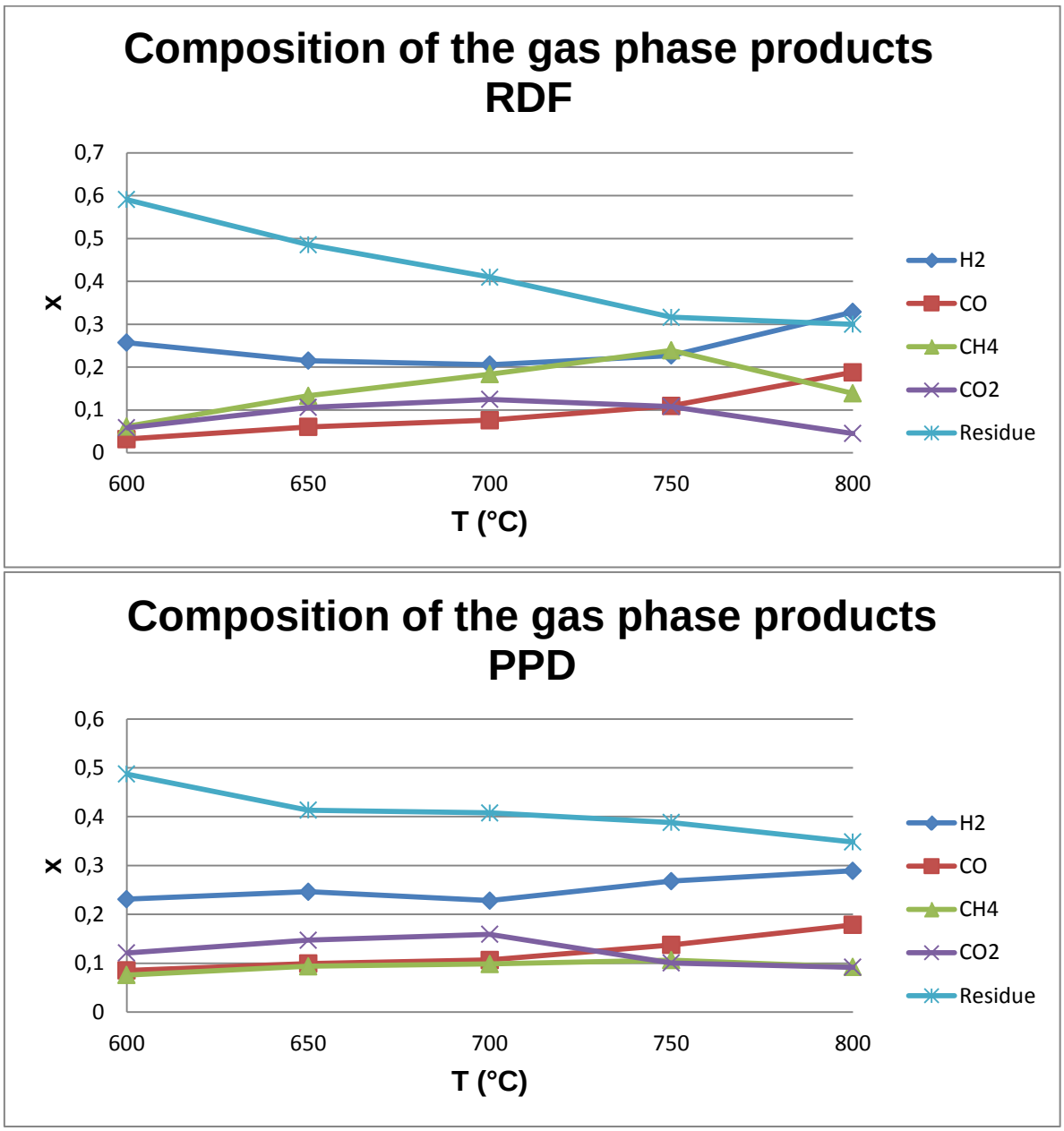

Figure 33. Relation between H_2, CO, CH_4, CO_2 and residue contents of the gas phase products and temperature for RDF and PPD. X represents the weight fraction.

As can be seen in Figure 33, there is clear trend in each component evolution with temperature, similar for both mixtures RDF and PPD. While some components like CO_2, CH_4 and H_2 present a more or less parabolic trend, there is a clear linear trend for increasing CO content (due to the enhancement of decarboxylation and decarbonylation reactions) and decreasing residue content with increasing temperature (Amutio et al., 2012). The reason why CO_2 content is higher at low temperatures is because it is produced by carboxyl release at those temperatures while CO and CH_4 are produced instead of CO_2 as the temperature increases due to secondary cracking of volatiles

(Coroson et al., 1989). Therefore, the optimal temperature in order to obtain less residue and CO_2 content, and more H_2, CO and relatively high CH_4 content either for RDF as for PPD is 800ºC. Carrying out the process at this temperature a higher quality gas is produced (high H_2 and CO content), a relatively high amount of CH_4 can be useful in order to produce calorific gas, and the emissions are more respectful with environment as there is lower amount of CO_2 and residue content. If the aim is the production of CH_4 then the more favorable temperature of operation is 750ºC, where for either RDF as for PPD the maximum content of CH_4 is produced. Finally, the overall less favorable temperature of operation is 700ºC, as there is the highest content of CO_2, the lowest content of H_2 and relatively low amount of CO content for RDF and PPD as well.

The results obtained here are confirmed for several other experiments already carried out (Figueroa et al., 2013; Amutio et al., 2012; Jasminská et al., 2013; Fu et al., 2011).

3.4.3. Thermal characterization of pyrolysis products

A thermal characterization of RDF and PPD char obtained from the first pyrolysis reactor has been done, in order to get more information which verifies the previously obtained results and furthermore to get new conclusions about pyrolysis process.

The thermal characterization consists on thermogravimetric analyses in order to find the ash content of the char output and calorimetric analyses in order to determine its combustion heat.

3.3.3.1. Thermogravimetric results

Thermogravietric analyses were set in order to find out the ash content of the char obtained from the first pyrolysis reactor. Experiments were set for RDF and PPD, for 600, 650, 700, 750 and 800ºC. In Table 25 results are shown, and the TG curves used to obtain the ashes results can be found in Appendix B.4.

	ASHES (%)	
TEMPERATURE	**RDF**	**PPD**
600	66,48	70,74
650	56,35	73,78
700	64,52	72,28
750	64,13	81,42
800	71,14	81,88

Table 25. Ash content of char from pyrolysis for RDF and PPD at 600, 650, 700, 750 and 800ºC. Values are expressed in percentage.

For a better understanding of the data in Table 25 and its dependence on temperature, Figure 34 shows a graph where the ash content in char is represented for each temperature.

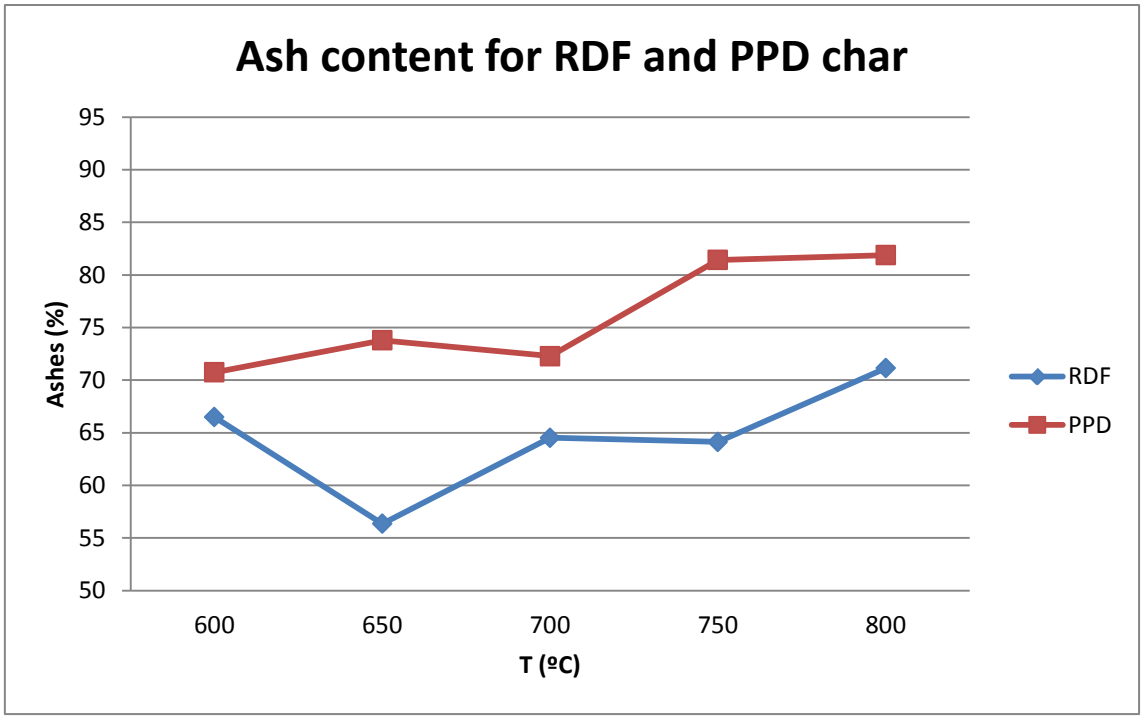

Figure 34. Graph representing ash content in RDF and PPD char depending on temperature.

As can be seen in Figure 34, ash content in PPD char present a clear trend to increase as temperature increases. It is caused by the volatile matter that is forcibly released of the char particles as the temperature has increased in the reactor and therefore less volatile matters are left in the particle from char. Moreover, at higher temperatures result into higher fixed carbon content and therefore there is less fixed carbon in char. All this produce a higher content of ashes in PPD char at higher temperatures (Parthanom et al., 2012). Therefore, the higher ashes content in PPD char is obtained at 800ºC.

However, behavior of ash content in RDF char depending on temperature is different than PPD. As it can be seen in Figure 34, there is an almost lineal trend for the RDF curve, which presents a maximum in ash content at 800ºC with 71,14%, and the lowest value (56,35%) at 650ºC. These results can be caused by the different composition between RDF and PPD. For RDF char fixed carbon and volatile fraction in char do not decrease at the same time like for PPD, as for RDF char volatile fraction increases while fixed carbon decreases as the temperature increases (Dou et al., 2007). Therefore the relation between the ash content on RDF char and the increasing temperature must not be a completely linear increase, as other researches, for example, have found that ash content decrease after 500ºC and increase again after 700ºC (Cozzani et al., 1995); for char from pyrolysis of used tires have been found that the maximum ash content on tar is at 550ºC and decreases after as the temperature increases (Popovic, 2000; Li et al., 2005). Due to this different results obtained by several investigations, it can be concluded that the waste used, its composition, the type of reactor used and the parameters set in it are very influential in RDF results. In this case, the temperature conditions where higher ash content from RDF char is obtained (which means that during pyrolysis process it releases higher volatile fraction) are 800ºC.

3.3.3.2. Calorimeter results

Calorimetric analyses have been also carried out in order to find out the combustion heat of PDF and RDF char obtained from pyrolysis process at 600, 650, 700, 750 and 800ºC. This way the remaining combustion heat of char will be obtained taking into account that the difference with the combustion heat in the input has been taken by the pyrolysis products.

In Table 26 results from calorimetric analyses are shown, while the original results obtained from the calorimetric analysis are shown in Appendix B.5.

MATERIAL	TEMPERATURE (ºC)	COMBUSTION HEAT (MJ/kg)
RDF	600	7,96
	650	7,80
	700	6,83
	750	8,47
	800	7,95
PPD	600	9,72
	650	7,44
	700	9,32
	750	9,32
	800	6,84

Table 26. Combustion heat of RDF and PPD char from pyrolysis process at 600, 650, 700, 750 and 800ºC.

In order to see easily the data in Table 26 and its dependence on temperature, Figure 35 shows a graph where the combustion heat of PPD and RDF char is represented for each temperature.

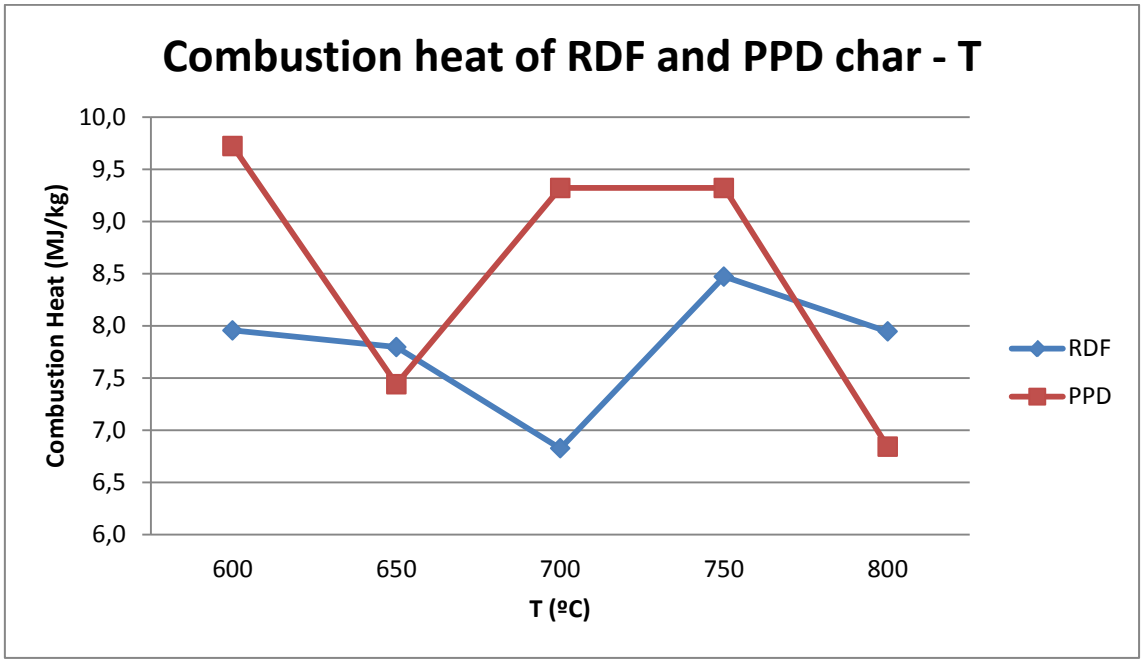

Figure 35. Graph representing the dependence between combustion heat of RDF and PPD char and temperature.

As it can be seen in Figure 35, combustion heats of PPD char at these temperatures are usually higher than combustion heats of RDF char. Carrying out an average between the content of textile, paper, HDPE, LDPE, PU and PS in RDF and PPD and the combustion heat of each content (which was measured during the thermal characterization of MSW), it is possible to obtain the proximate combustion heat of each mixture: 23 MJ/kg for RDF and 28,66 MJ/kg for PPD. Therefore is not strange that PPD char combustion heats are higher than for RDF char. Moreover, considering an average of PPD and RDF char combustion heats, the heating value carried by pyrolysis products can be approximated by the difference with the combustion heat of the input; the heating value difference for RDF is 15,20 MJ/kg, and 20,13 MJ/kg by PPD. Therefore, products from PPD pyrolysis may have higher heating value.

In Figure 35 can be seen how at 800ºC PPD char reaches its lowest combustion heat and at 600ºC its maximum. RDF char reaches its maximum combustion heat at 750ºC and its lowest at 800ºC. There is no trend in any mixture, unlike what several pyrolysis researches which have been carried out previously sustain, it should be an increase in the char combustion heat as the temperature increase (Ragauskas, 2014; Demirbas, 2004). Nevertheless, the increase of combustion heats of char in those researches are usually few, as the combustion heat values of char during increasing temperature are very similar. The maximum difference between combustion heat is 3 MJ/kg, which it can be produced because of several reasons (little deviation in the pyrolysis process, removal of char with some previous char fraction, little human error while sorting waste, etc.).

3.5. Conclusions

After all results have been presented and discussed, further conclusions can be extracted. The objective of this thesis was the characterization of MSW (the input of MSW and the outputs from its pyrolysis) for purpose of its gasification and pyrolysis. The objective has been reached leading to conclusions about the the best operating conditions to obtain the wanted results with different MSW mixtures.

First, as far as initial RDF and PPD input characterization is concerned, it has been seen as the RDF produces more tar due to its paper content (which after pyrolysis generate complex hydrocarbons derived from cellulose such as avicel, levoglucosan, acetates, and alkaline salts) (Evans et al., 2006) but more non-condensable gases due to its high LDPE content mainly carbon and hydrogen (Kaminsky, 1993; CDS, 2009; CDS, 2014). Moreover, the H_2 and CH_4 content of those non-condensable gases is overall higher for RDF and there is also more CO content if pyrolysis is carried out at high temperatures, the overall CO_2 content is lower, but the residue of non-condensable gases content is higher for RDF too. The ash content analysis from char output reflect higher ash content for PPD char, which usually means a higher volatile fraction released (Parthanom et al., 2012). Nevertheless, much more char is generated with PPD so there is less tar and non-condensable gases. Therefore, if the objective is aimed at obtain the higher H_2 and CO overall production, and less CO_2 overall production, the most favorable condition is a

high temperature pyrolysis, as H_2 and CO increase, and tar and CO_2 decreases as the temperature increases. The best temperature conditions in furnaces are 800ºC. Furthermore, at this temperature the amount of CH_4 obtained is high despite not being the maximum.

On the other hand, a high heating value difference between input sample and output char may be also desired, in order to get higher heating values for product gases. In this way, RDF and PPD mixtures have been obtained by sorting the different MSW components in order to achieve a higher combustion heat. Nevertheless, there is a significant difference between both, as by calorimetric experiments with the RDF and PPD char produced by pyrolysis and thermogravimetric experiments with the input mixtures, has been found that initial PPD mixture has a higher combustion heat compared to RDF mixture and, moreover, studying the difference with the remaining combustion heat in char it can be seen that this difference is higher for PPD mixture. Therefore, in order to obtain gases with higher heating values the most favorable process conditions are focused on setting the furnaces at higher temperatures (at 800ºC there is the higher heating difference for PPD).

Finally, as a recommendation for future researches, the most influential parameters have been the MSW composition and the process temperature, so future experiments should be focused on optimization between an improved MSW components sorting and the temperature set during process, in order to get higher amount of gases (with higher content of H_2, CO and CH_4) and higher products heating values. This way, maybe in a not so distant future pyrolysis will be a viable and reliable process to take profit from municipal solid waste removing it at the same time as energy is produced, in a large-scale plant.

Appendices

Appendix A – Introduction

Further information of MSW production in the world and particularly in Europe is represented in Figure 36 and Figure 37.

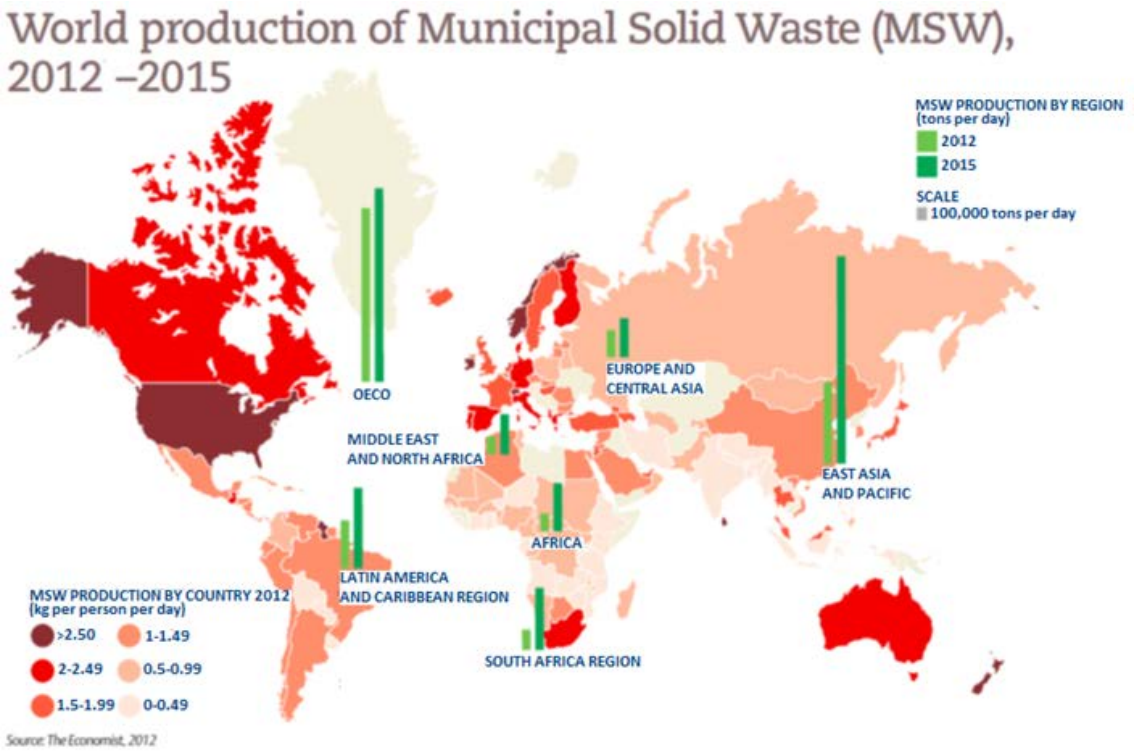

Figure 36. World production of MSW, 2012-2015 (Popraco, 2012, Source: The World Bank, 2012).

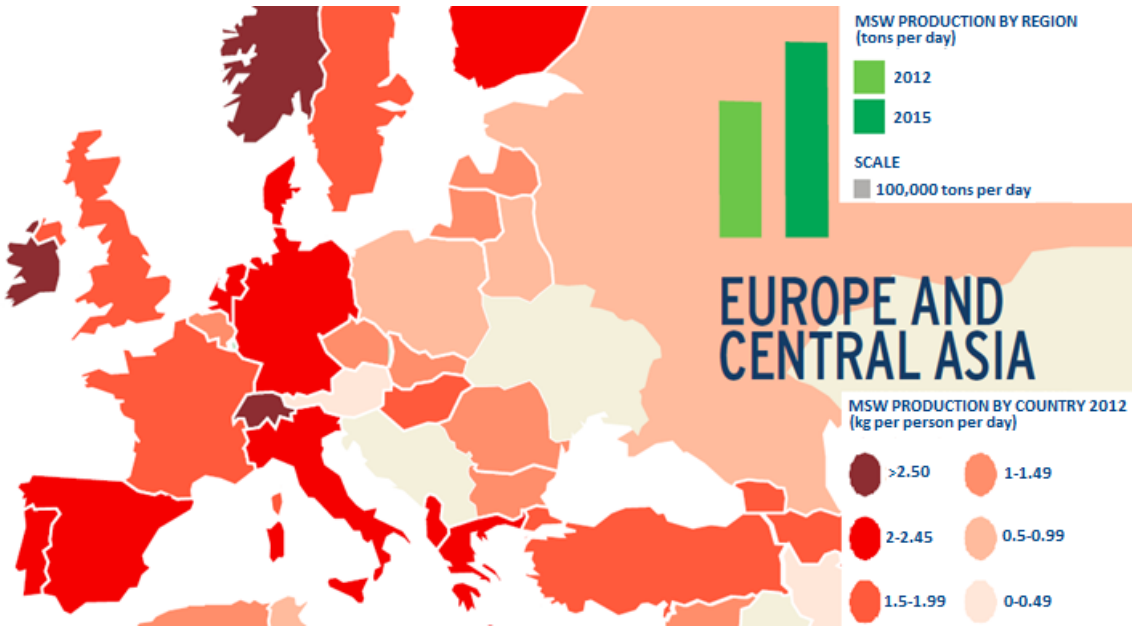

Figure 37. Europe and Central Asia production of MSW, 2012-2015 (Popraco, 2012, Source: The World Bank, 2012).

In Figure 36 and Figure 37 it is represented the production of MSW in 2012 as well as the estimation for 2015.

Moreover, in Figure 38 it can be seen a graph where are represented the fractions of MSW disposed for landfilling, composting and incineration for each European country.

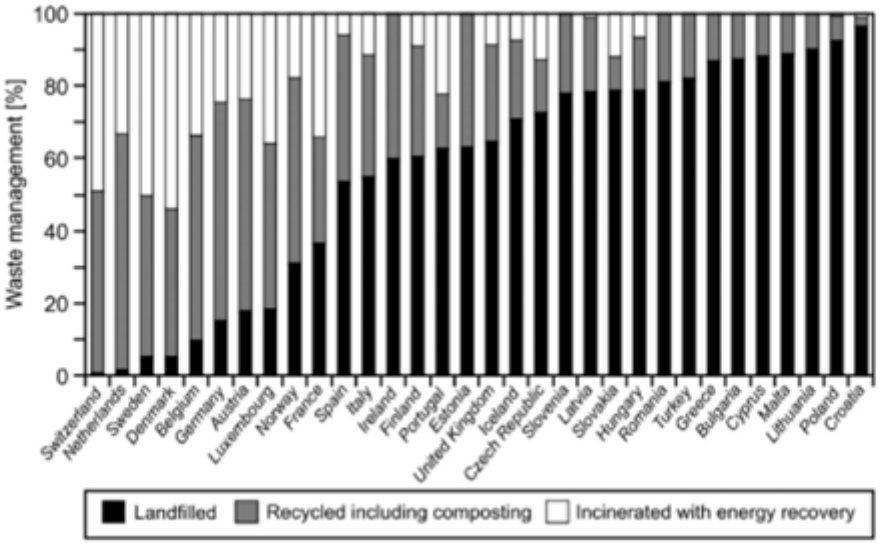

Figure 38. Residential waste management in Europe based on data from Eurostat 2007 (ETC/WRM, 2002).

Appendix B – Experimental Data

Appendix B.1 – TG curves of MSW components

In this appendix the curves obtained from thermogravimetric experiments of each MSW component are given. These curves consist on a curve which represents the decrease of mass along with the time (which is associated with the temperature increase), and the derivative curve for each point of the curve. The derivative curve is needed to find out the moisture content (as there is a little minimum at the beginning of the derivative curve when moisture is released). The ash content is represented by the final value of the curve, the fixed carbon is the mass percentage difference in the last sudden step, and the volatile fraction has been found by the difference between 100 and the sum of the other fractions. This way, the proximate analysis is carried out and, along with the elemental analysis results, the elemental analysis can be obtained too.

In order to show only one TG curve example for each component, only curves obtained with a 20ºC/min heating rate have been given.

Textile TG curve

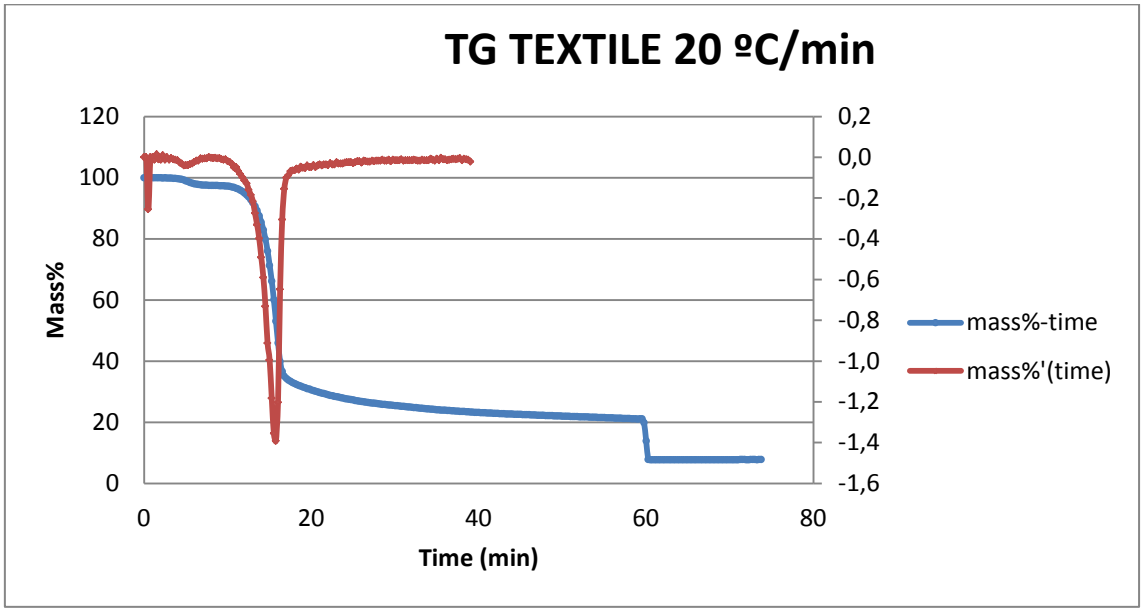

Figure 39. TG curve of textile carried out with a 20ºC/min heating rate. The blue line represents the decrease of mass percentage along with the time. The red line is the derivative curve.

For textile curve is easy to see the moisture step at the beginning (where there is a little minimum of the derivative curve), the final ash content value, the fixed carbon step (the last sudden step in blue line) and the volatile fraction release (where there is a big minimum of the derivative curve).

In Table 27 the values of the proximate analysis for this curve are shown.

TOTAL	mass%
Moisture	2,47
Volatile content	76,39
Fixed carbon	13,31
Ashes	7,82

Table 27. Proximate analysis of textile TG curve carried out with a 20ºC/min heating rate.

Polystyrene TG curve

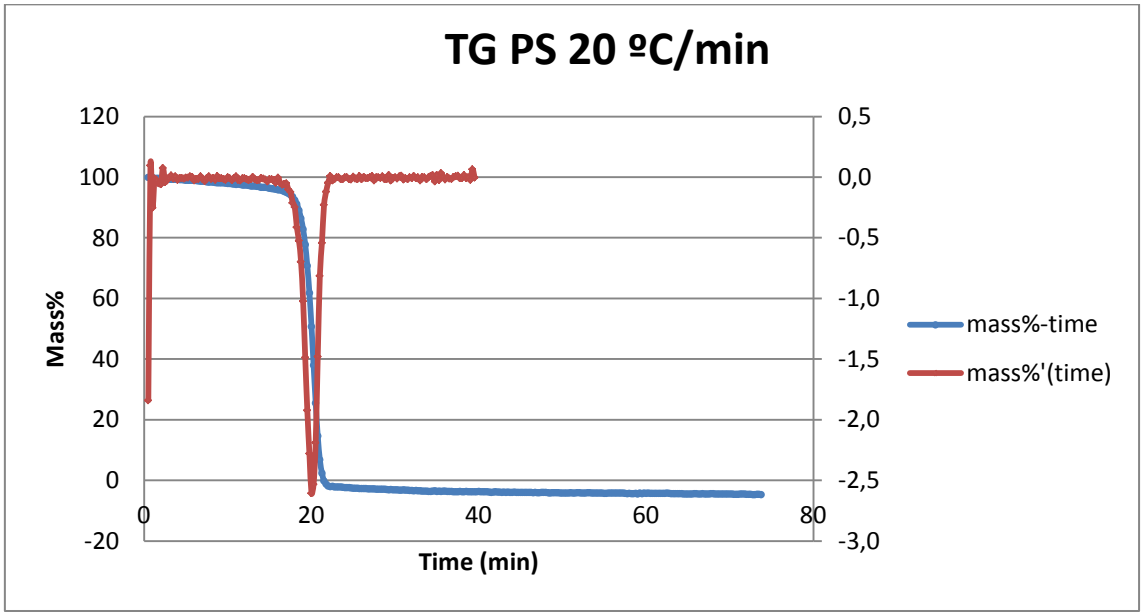

Figure 40. TG curve of polystyrene (PS) carried out with a 20ºC/min heating rate. The blue line represents the decrease of mass percentage along with the time. The red line is the derivative curve.

As it can be seen in Figure 40, PS is composed only for volatile fraction.

LDPE TG curve

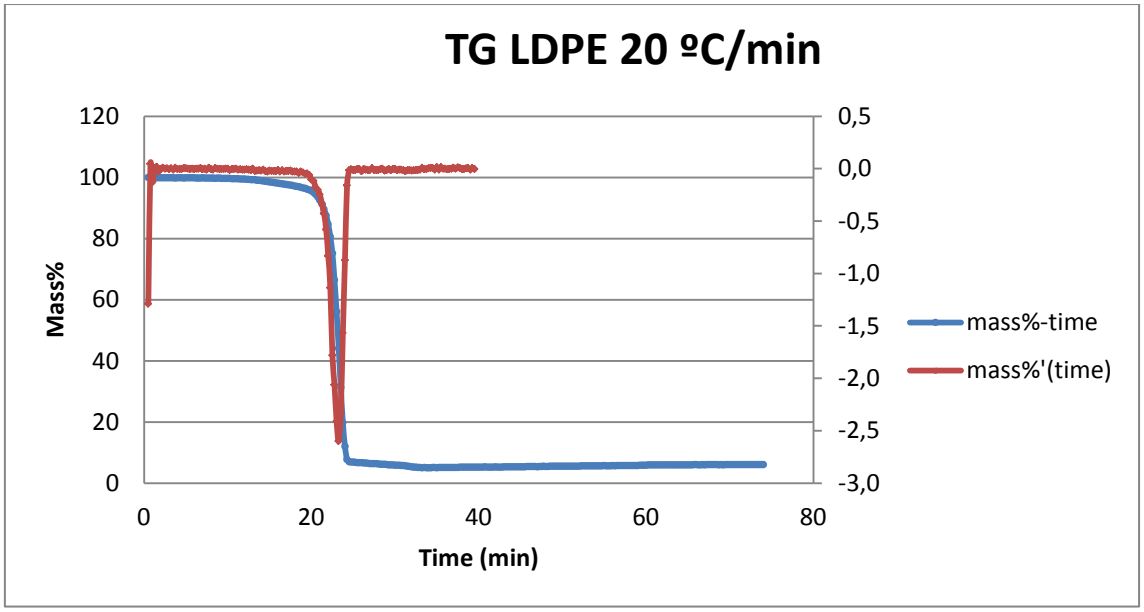

Figure 41. TG curve of low density polyethylene (LDPE) carried out with a 20ºC/min heating rate. The blue line represents the decrease of mass percentage along with the time. The red line is the derivative curve.

In Figure 41 it is shown how LDPE is composed only for volatile fraction and a few content of ashes. In Table 28 the values of the proximate analysis for this curve are shown.

TOTAL	mass%
Volatile fraction	94,95
Ashes	5,05

Table 28. Proximate analysis of LDPE TG curve carried out with a 20ºC/min heating rate.

White Paper TG curve

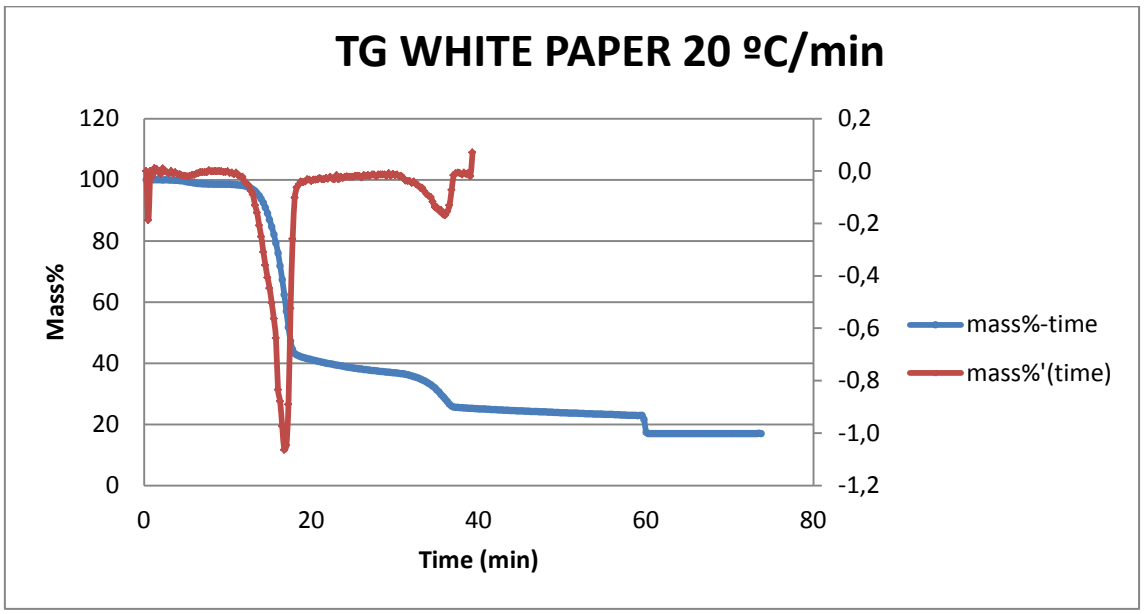

Figure 42. TG curve of white paper carried out with a 20ºC/min heating rate. The blue line represents the decrease of mass percentage along with the time. The red line is the derivative curve.

In Figure 42 the curve which represents the decrease of the mass percentage as the time goes by presents three different steps during volatile fraction is released. This is because of the three main components of paper: cellulose, hemicellulose and lignin. Those three components have different chemical structure and different degradation rate. Lignin is difficult to degrade and therefore it starts to degrade slowly until it reaches high temperatures when it is totally degraded. On the other hand, hemicellulose undergoes a fast degradation at low temperatures while cellulose degrades at temperatures around 325ºC and 375ºC (Blasi, 2008). Therefore, in the first step mainly hemicellulose is degraded while lignin is starting to degrade; in the second step mainly cellulose undergoes degradation along with a slow degradation of lignin; and in the third step lignin is totally degraded (Burhenne et al., 2013).

In Table 29 the values of the proximate analysis for this curve are shown.

TOTAL	mass%
Moisture	1,29
Volatile fraction	75,72
Fixed carbon	5,97
Ashes	17,02

Table 29. Proximate analysis of white paper TG curve carried out with a 20ºC/min heating rate.

Recycled Paper TG curve

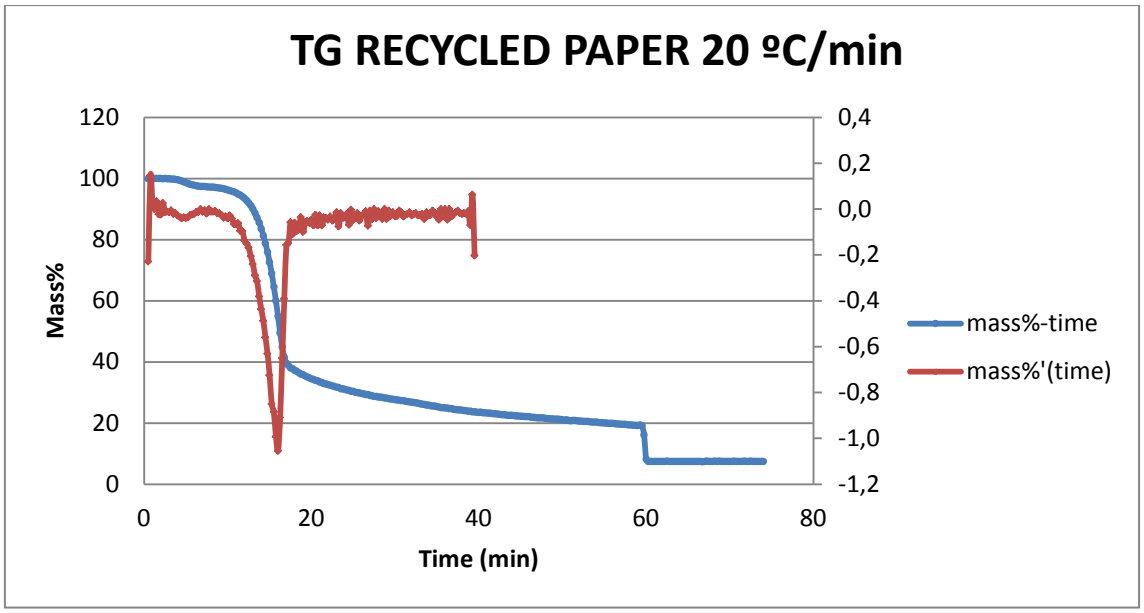

Figure 43. TG curve of recycled paper carried out with a 20ºC/min heating rate. The blue line represents the decrease of mass percentage along with the time. The red line is the derivative curve.

Figure 43 presents a different curve with respect to white paper, as there are not three clear steps when volatile fraction is released despite having similar chemical composition to white paper, containing hemicellulose, cellulose and lignin too. In this case, there is only one unique step for volatile fraction.

In Table 30 the values of the proximate analysis for this curve are shown.

TOTAL	mass%
Moisture	2,79
Volatile fraction	78,07
Fixed carbon	11,74
Ashes	7,40

Table 30. Proximate analysis of recycled paper TG curve carried out with a 20ºC/min heating rate.

HDPE TG curve

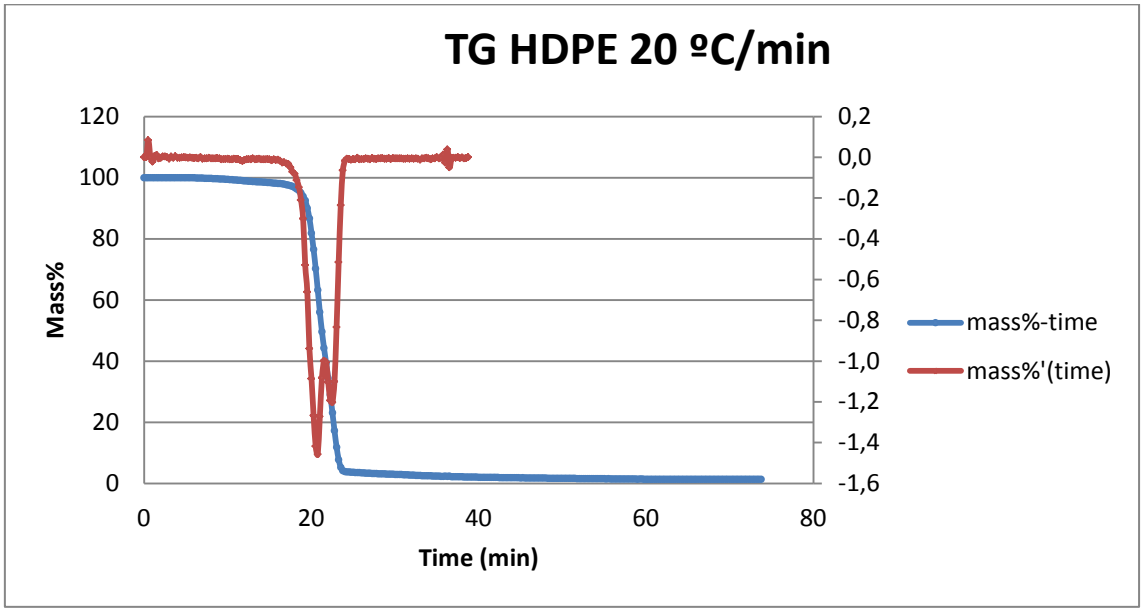

Figure 44. TG curve of high density polyethylene (HDPE) carried out with a 20ºC/min heating rate. The blue line represents the decrease of mass percentage along with the time. The red line is the derivative curve.

As for LDPE thermogavrimetric curve, the composition of HDPE is mainly volatile fraction with a low content of ashes. In Table 31 the values of the proximate analysis for this curve are shown.

TOTAL	mass%
Moisture	0
Volatile content	98,62
Fixed carbon	0
Ashes	1,38

Table 31. Proximate analysis of recycled paper TG curve carried out with a 20ºC/min heating rate.

Polyurethane TG curve

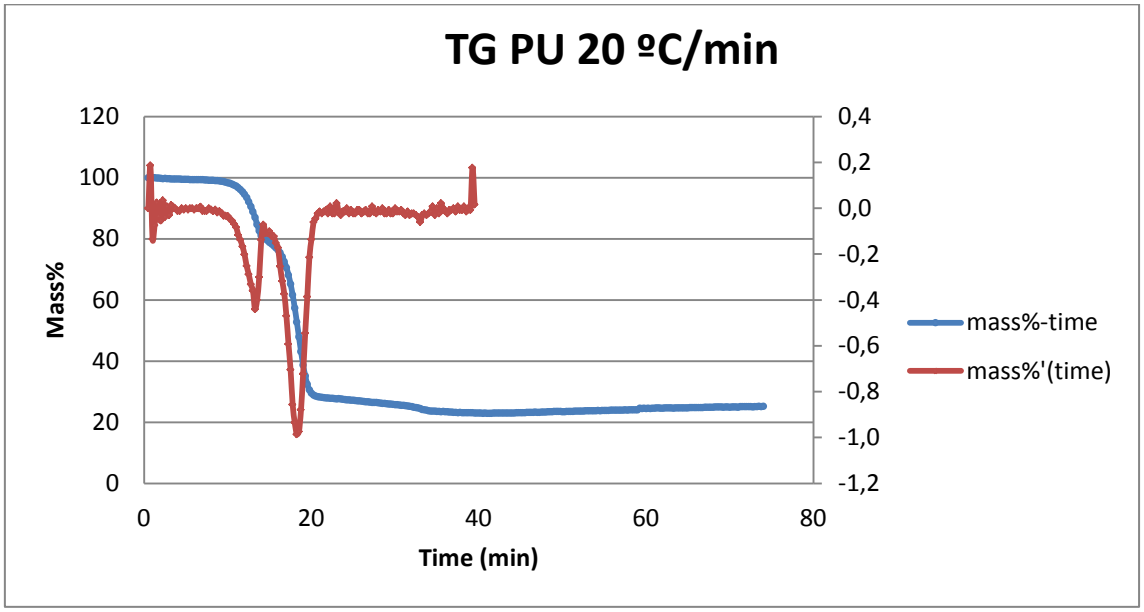

Figure 45. TG curve of polyurethane (PU) carried out with a 20ºC/min heating rate. The blue line represents the decrease of mass percentage along with the time. The red line is the derivative curve.

In Figure 45 can be seen as when volatile fraction is released there is a small step at the beginning and a second larger step. This can be caused by a non-pure PU sample, which can contain little fractions of other plastics.

In Table 32 the values of the proximate analysis for this curve are shown.

TOTAL	mass%
Moisture	0
Volatile content	77,05
Fixed carbon	0
Ashes	22,95

Table 32. Proximate analysis of polyurethane (PU) TG curve carried out with a 20ºC/min heating rate.

Appendix B.2 – Results of calorimetric analysis from MSW components

In Table 33 the original results of the calorimetric analysis from MSW components are given. Two calorimetric experiments were carried out for each component, so for the thesis analysis an average of every two values was calculated.

	Combustion Heat (MJ/kg)	
MATERIAL	**Value 1**	**Value 2**
PU	19,43	23,68
TEXTILE	21,39	19,77
PS	41,44	42,73
HDPE	33,57	35,83
White Paper	13,41	14,57
Recycled Paper	14,62	14,54
LDPE	44,22	43,86

Table 33. Original results obtained from the calorimetric analysis of MSW components.

It can be seen as the results from both experiments are very similar, so the average between them can be calculated.

Appendix B.3 – TG curves of RDF and PPD mixtures

Thermogavrimetic curves of RDF and PPD mixtures where used in order to get the proximate analysis of each mixture. Those experiments with thermogravimetric analyzer were carried out only with one heating rate, the same for both mixtures: 10ºC/min.

In Figure 46 and Figure 47 TG curves of RDF and PPD mixtures are represented. The lines represented in the graphs have the same meaning as for MSW components TG curves.

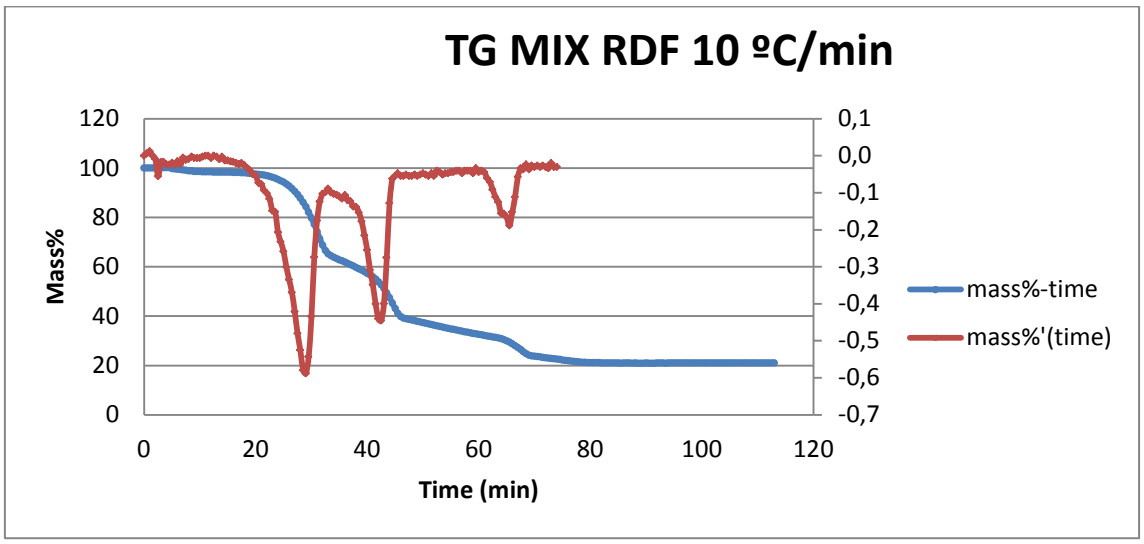

Figure 46. TG curve of RDF mixture carried out with a 10ºC/min heating rate. The blue line represents the decrease of mass percentage along with the time. The red line is the derivative curve.

In Table 34 the values of the proximate analysis for this curve are shown.

TOTAL	mass%
Moisture	1,33
Volatile content	77,66
Fixed carbon	0
Ashes	21,01

Table 34. Proximate analysis of RDF mixture TG curve carried out with a 10ºC/min heating rate.

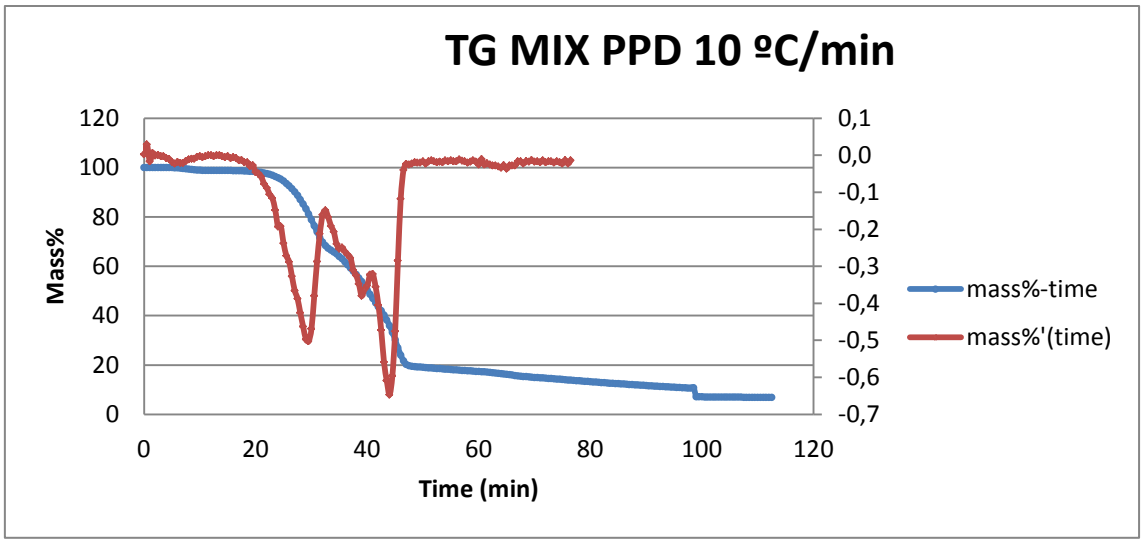

Figure 47. TG curve of PPD mixture carried out with a 10ºC/min heating rate. The blue line represents the decrease of mass percentage along with the time. The red line is the derivative curve.

In Table 35 the values of the proximate analysis for this curve are shown.

TOTAL	mass%
Moisture	1,15
Volatile content	88,13
Fixed carbon	3,74
Ashes	6,97

Table 35. Proximate analysis of PPD mixture TG curve carried out with a 10ºC/min heating rate.

Appendix B.4 – TG curves of RDF and PPD char

In order to find the final ash content of RDF and PPD char, thermogravimetric curves of each mixture char obtained from pyrolysis at 600, 650, 700, 750 and 800ºC were used. All the thermogravimetric experiments were carried out at 20ºC/min heating rate. As there are several curves, for better understanding of the difference between each TG curve with the temperature, they have been represented in two graphs, Figure 48 and Figure 49, representing all curves at different temperature of the same mixture chars in the same figure.

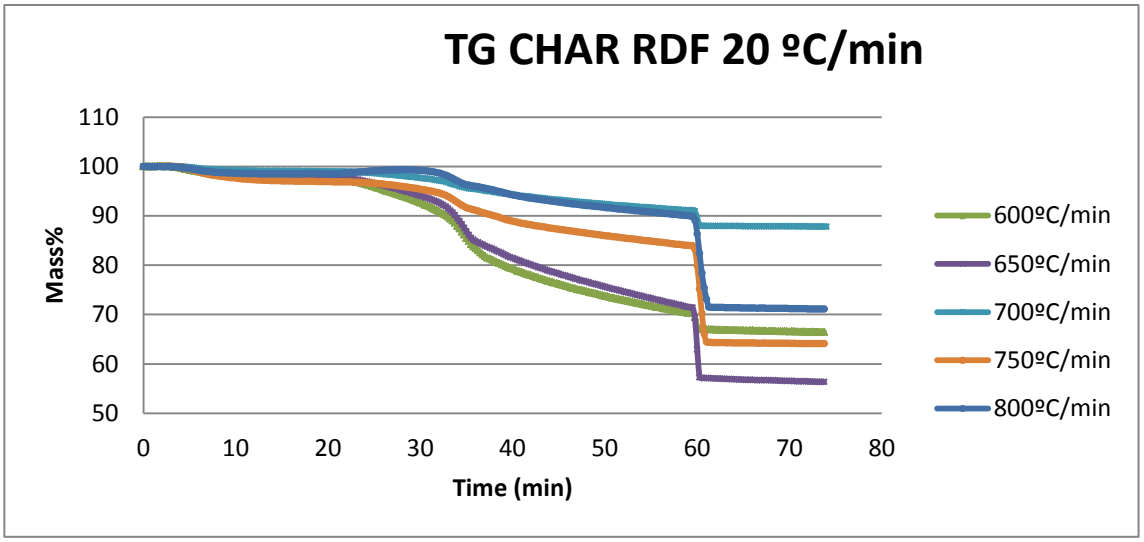

Figure 48. TG curves of RDF char from pyrolysis carried out at 20ºC/min heating rate. The blue line represents the decrease of mass percentage along with the time. The red line is the derivative curve.

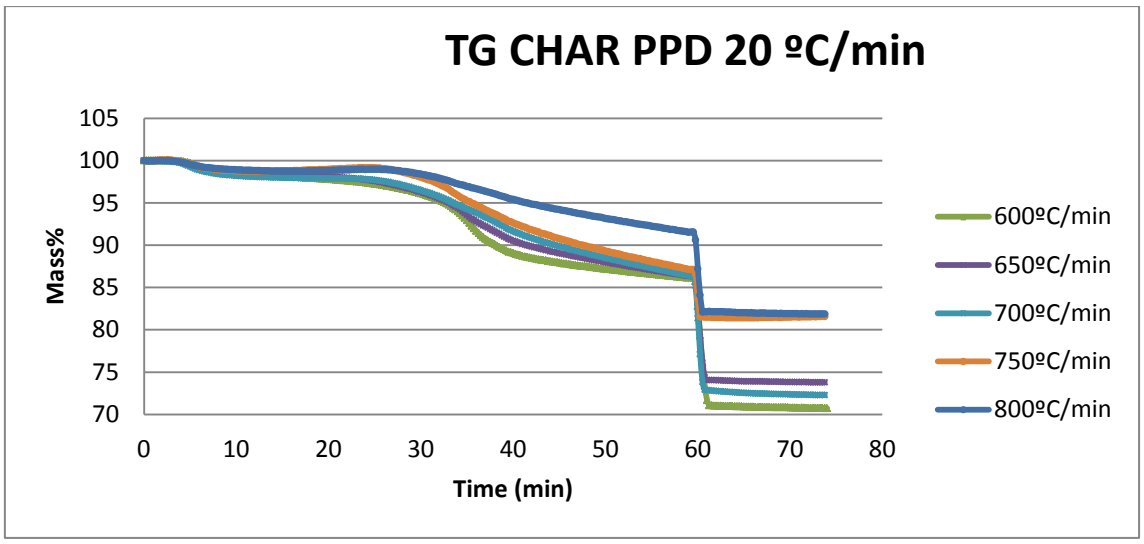

Figure 49. TG curves of PPD char from pyrolysis carried out at 20ºC/min heating rate. The blue line represents the decrease of mass percentage along with the time. The red line is the derivative curve.

In Figure 48 and Figure 49 is easy to see like with the ashes analysis the evolution of the TG curve with the increasing temperature. As has been said previously on the ashes results discussion, PPD char TG curves follow the trend to undergo a lower mass percentage decrease as the temperature increases, while there is not a clear trend for RDF char TG curves.

Appendix B.5 – Results of calorimetric analysis from RDF and PPD char

In Table 36 the original results of the calorimetric analysis from RDF and PPD char are given. Two calorimetric experiments were carried out for each mixture char obtained from pyrolysis at 600, 650, 700, 750 and 800ºC, so for the thesis analysis an average of every two values was calculated.

		COMBUSTION HEAT (MJ/kg)	
MATERIAL	**TEMPERATURE**	**Value 1**	**Value 2**
RDF	600	7,25	8,66
	650	7,28	8,31
	700	7,10	6,55
	750	8,83	8,11
	800	12,49	15,52
PPD	600	9,32	10,12
	650	6,34	8,54
	700	9,55	9,09
	750	10,42	8,22
	800	7,81	5,87

Table 36. Original results obtained from the calorimetric analysis of RDF and PPD char.

As can be seen in Table 36, each two different values of combustion heat are very similar, so the average between them can be calculated.

References

I. Aigner, U. Wolfesberger and H.Hofbauer (2009). Tar Content and Composition in Producer Gas of Fluidized Bed Gasification and Low Temperature Pyrolysis of Straw and Wood–Influence of Temperature. International Conference on Polygeneration Strategies (ICPS), 2009.

A. C. Aiken, P. F. DeCarlo and J. L. Jimenez (2007). Elemental Analysis of Organic Species with Electron Ionization High-Resolution Mass Spectrometry. Analytical Chemistry 79, 2007, 8350-8358.

M. N. Almustapha and J. M. Andresen (2011). Catalytic Conversion of High Density Polyethylene (HDPE) Polymer as a means of recovering valuable energy content from the plastic wastes. IPCBEE (International Proceedings of Chemical, Biological and Environmental Engineering), volume 26, 2011.

M. Amutio, G. Lopez, M. Artetxe, G. Elordi, M. Olazar and J. Bilbao (2012). Influence of temperature on biomass pyrolysis in a conical spouted bed reactor. Resources, Conservation and Recycling 59, 2012, 23-31.

U. Arena (2011). Process and technological aspects of municipal solid waste gasification. A review. Waste Management 32, 2011, 625-639.

U. Arena and M. L. Mastellone (2005). Fluidized Pyrolysis and Gasification of Solid Wastes, in Proc. of Industrial Fluidization South Africa 2005, The South African. Institute of Mining and Metallurgy. ISBN 1-919782-83-0, pp. 53-68.

U. Arena and M. L. Mastellone (2009). Fluidized bed gasification of RDF and PDF. AMRA Scientific Report. ISBN 978-88-89972-10-6 (in Italian, with an executive summary in English). Available on <www.amracenter.com>.

M. P. Aznar, M. A. Caballero, J. Gil, J. A. Martin and J. Corella (1998). Commercial steam reforming catalysts to improve biomass gasification with steam-oxygen mixtures. 2. Catalytic tar removal. Industrial & Engineering Chemistry Research 37, 1998, 2668-2680.

E. G. Baker, L. K. Mudge and W. A. Wilcox (1996). Proceedings of Conference on Developments in Thermochemical Biomass Conversion. Banff, Canada, 1996, pp. 305-314.

D. N. Bangala, N. Abatzoglou and E. Chornet (1998). Steam reforming of naphthalene on Ni-Cr/Al2O3 catalysts doped with MgO, TiO_2, and La_2O_3. American Institute of Chemical Engineers (AIChE) Journal 44, 1998, 927-936.

V. Belgiorno, G. De Feo, C. Della Rocca and R. M. A. Napoli (2003). Energy from gasification of solid wastes. Waste Management 23, 2003, 1-15.

B. Bilitewski, G. Härdtle, K. Marek, A. Weissbach and H. Boeddicker (1997). Waste Management. Springer-Verlag, Heidelberg, Germany, 1997. ISBN 3-540-59210-5.

C. D. Blasi (2008). Modeling chemical and physical processes of wood and biomass pyrolysis. Progress in Energy and Combustion Science 34, 2008, 47-90.

M. Boroson, J. Howard, J. Longwell and W. Peters (1989). Product yields and kinetics from the vapor-phase cracking of wood pyrolysis tars. American Institute of Chemical Engineers (AIChE) Journal 35, 1989, 120-128.

A. Bridgwater, D. Meier and D. Radlein (1999). An overview of fast pyrolysis of biomass. Organic Geochemistry 30, 1999, 1479-1493.

L. Burhenne, J. Messmer, T. Aicher and M.-P. Laborie (2013). The effect of the biomass components lignin, cellulose and hemicellulose on TGA and fixed bed pyrolysis. Journal of Analytical and Applied Pyrolysis 101, 2013, 177-184.

CDS (CDS Analytical, Inc.) (2009). Capillary GC of polyolefin pyrolysates. CDSolutions, 2009. Available on <http://www.analytix.co.uk/Products/Pyrolysis/CDS_pyrolysis_applications/Capillary_GC_of_polyolefin_pyrolysates.pdf>.

CDS (CDS Analytical, Inc.) (2014). Evolved Gas Analysis of a Polyurethane Foam. CDSolutions, 2014. Available on <http://www.analytix.co.uk/Products/Pyrolysis/CDS_pyrolysis_applications/142_Evolved_gas_analysis_of_a_polyurethane_foam.pdf>.

T. H. Christensen, T. Hulgaard, J. Vehlow, S. Dalager, O. Hjelmar, A. Johnson, R. Comans, H. Rechberger, S. Rotter, T. Astrup, B. Bilitewski, E. Stentiford, M. de Bertoldi, U. Krogmann, I. Körner, L. F. Diaz, H. Scharff, S. Manfredi, P. Kjeldsen et al. (2011). Solid Waste Technology and Management, volume 1 and 2, edited by T. H. Christensen, 2011. ISBN 978-1-405-17517-3, pp. 365-695.

J. Corella, M. P. Aznar, J. Delgado, M. P. Martinez and J. L. Aragües (1991). The deactivation of tar cracking stones (dolomites, calcites, magnesites) and of commercial methane steam reforming catalysts in the upgrading of the exit gas from steam fluidized bed gasifiers of biomass and organic wastes. Studies in Surface Science and Catalysis 68, 1991, 249-52.

V. Cozzani, C. Nicolella, L. Petarca, M. Rovatti and L. Tognotti (1995). A Fundamental Study on Conventional Pyrolysis of a Refuse-Derived Fuel. Industrial & Engineering Chemistry Research 34, 1995, 2006-2020.

G. De Feo, V. Belgiorno, R. M. A. Napoli and U. Papale (2000). Solid Wastes Gasification. SIDISA International Symposium on Sanitary and Environmental Engineering, 2000.

C. Della Rocca (2001). I processi e le tecnologie di gassificazione delle biomasse e dei rifiuti solidi. Civil Engineering Degree Thesis, Università degli Studi di Salerno, 2001.

A. Demirbas (2004). Determination of calorific values of bio-chars and pyro-oils from pyrolysis of beech trunkbarks. Journal of Analytical and Applied Pyrolysis 72, 2004, 215-219.

B. Dou, S. Park, S. Lim, T.-U Yu and J. Hwang (2007). Pyrolysis Characteristics of Refuse Derived Fuel in a Pilot-Scale Unit. Energy and Fuels 21, 2007, 3730-3734.

EC (European Commission), Directorate General Environment (2003). Refuse derived fuel, current practice and perspectives (B4-3040/2000/306517/MAR/E3), final report, July 2003.

EPA (United States Environmental Protection Agency) (2012). Waste - Non-Hazardous Waste - Municipal Solid Waste, 2012. Available on <http://www.epa.gov/osw/nonhaz/municipal/>.

ETC/WRM (European Topic Center for Waste and Resource Management) (2002). Reprinted with impression from Final report to the Directorate General Environment, Costs for municipal waste management in the EU by D. Hogg ©, European Commission, 2002. Available on <http://ec.europa.eu/environment/waste/pdf/final_report_10042012.pdf>.

R. J. Evans, E A. Agblevor, H. L. Chum, J. B. Wooten, D. B. Chadwick and S. D. Baldwin (2006). New approaches to the study of cellulose pyrolysis, 2006, pp. 714-724.

FAA (Federal Aviation Administration, United States) (2001). Molar Group Contributions to the Heat of Combustion (DOT/FAA/AR-TN01/75). National Technical Information Service (NTIS), 2001. Available on <http://www.tc.faa.gov/its/worldpac/techrpt/artn01-75.pdf>.

V. P. Fadeeva, V. D. Tikhova and O. N. Nikulicheva (2007). Elemental Analysis of Organic Compounds with the Use of Automated CHNS Analyzers. Journal of Analytical Chemistry 63, 2008, 1094–1106.

J. E. J. Figueroa, Y. Camacho Ardila, B. Hoss Lunelli, R. Maciel Filho and M. R. Wolf Maciel (2013). Evaluation of Pyrolysis and Steam Gasification Processes of Sugarcane Bagasse in a Fixed Bed Reactor. Chemical Engineering Transactions, volume 32, 2013. ISBN 978-88-95608-23-5.

Friends of the Earth (2002). Pyrolysis and Gasification, 2002. Available on<https://mysite.wsu.edu/personal/gmwaniki/biofuels/Related%20documents/gasification_pyrolysis.pdf>.

P. Fu, W. Yi, X. Bai, Z. Li, S. Hu and J. Xiang (2011). Effect of temperature on gas composition and char structural features of pyrolyzed agricultural residues. Bioresource Technology 102, 2011, 8211-8219.

J. F. González, S. Román, G. Engo, J. M. Encinar and G. Martínez (2011). Reduction of tras by dolomite cracking during two-stage gasification of olive cake. Biomass and bioenergy 35, 2011, 4324-4330.

W. B. Hauserman, N. Giordano, M. Laganà and V. Recupero (1997). Biomass gasifiers for fuel cells systems. La Chimica & L'Industria 2, 1997, 199–206.

M. He, Z. Hu, B. Xiao, J. Li, X. Guo and S. Luo et al. (2009). Hydrogen-rich gas from catalytic steam gasification of municipal solid waste (MSW): influence of catalyst and temperature on yield and product composition. International Journal of Hydrogen Energy 34, 2009, 195-203.

Hope College, Holand (2000). Bomb calorimetry, 2000. Available on <http://www.chem.hope.edu/~polik/Chem345-2000/bombcalorimetry.htm>.

M. R. Islam, A. B. Chhetri and M. M. Khan (2011). Greening of Petroleum Operations: The Science of Sustainable Energy Production. ISBN 978-0-470-62590-3.

İTÜ (Istanbul Technical University) (2011). Fen Edebiyat Fakültesi Polimer Bilimi ve Teknolojisi, Ana Bilim Dalı 34469 Maslak / İSTANBUL. PST 522E - Synthesis and Characterization of Macromolecules, Chapter 12: Thermogravimetric Analysis, 2011.

JAEE (Japanese Advanced Environment Equipment) (2011). Mitsui Recycling 21 Pyrolysis Gasification and Melting Process for Municipal Waste. Available on <www.gec.ip/JSIM_DATA/WASTE/WASTE_3/html/Doc_436.html>.

N. Jasminská, T. Brestovič and M. Čarnogurská (2013). The Effect of Temperature Pyrolysis Process of Used Tires on the Quality of Output Products. Acta Mechanica et Automatica 7, 2013, 20–25.

Juniper (2001). Pyrolysis and gasification of waste: a worldwide technology and business review, volume 2, 2001. Technology and processes, 2nd edition. Juniper Consultancy Services Ltd, Stancombe, UK.

W. Kaminsky (1993). Recycling of polymers by pyrolysis. Colloque C7, supplément au Journal de Physique 111, volume 3, 1993.

H. Karatas, H. Olgun, F. Akgun (2012). Coal and coal and calcined dolomite gasification experiments in a bubbling fluidized bed gasifier under air atmosphere. Fuel processing Technology 106, 2013, 666-672.

I. Kayacan and Ö. M. Dogan (2008). Pyrolysis of Low and High Density Polyethylene. Part I: Non-isothermal Pyrolysis Kinetics. Energy Sources 30, 2008, 385-391.

A. Klein, K. Whiting, E. Archer and J. Schwager (2004). Gasification and pyrolysis: what is the current situation for waste management? Waste Management World, 2004, pp. 71–75.

S. Li, Y. Lu, L. Guo and X. Zhang (1996). Hydrogen production by biomass gasification in supercritical water with bimetallic Ni-M/gAl2O3 catalysts (M = Cu, Co and Sn). International journal of hydrogen energy 36, 2011, 14391-14400.

S.-Q. Li, Q. Yao, S.-E. Wen, Y. Chi and J.-H. Yan (2005). Properties of Pyrolytic Chars and Activated Carbons Derived from Pilot-Scale Pyrolysis of Used Tires. Air & Waste Management Association 55, 2005, 1315-1326.

C. Li and K. Suzuki (2009). Tar property, analysis, reforming mechanism and model for biomass gasification - An overview. Renewable and Sustainable Energy Reviews 13, 2009, 594-604.

P. C. Lodi and B. de Souza Bueno (2012). Thermo-gravimetric Analysis (TGA) after Different Exposures of High Density Polyethylene (HDPE) and Poly Vinyl Chloride (PVC) Geomembranes. EJGE (Electronic Journal of Geotechnical Engineering), volume 17, 2012.

T. Malkow (2004). Novel and innovative pyrolysis and gasification technologies for energy efficient and environmentally sound MSW disposal. Waste Management 24, 2004, 53-79.

T. Milne, R. Evans and N. Abatzoglou (1998). Biomass Gasifiers "Tars": Their Nature, Formation, and Conversion. NREL (National Renewable Energy Laboratory), 1998. Available on <http://www.nrel.gov/docs/fy99osti/25357.pdf>.

Mineral Data Publishing, 2001-2005. Available on <http://rruff.info/doclib/hom/dolomite.pdf>.

J. P. A. Neeft (2005). Rationale for setup of impinger train as used in the Technical Specification of Sampling and Analysis of Tar and Particles in the Product Gases of Biomass Gasification. Technical background document CEN BT/TF 143 “Organic contaminants (“tar”) in biomass producer gases”, 2005. Available on <http://www.tarweb.net/>.

V. Nelson, Department of Agriculture and Rural Development, Government of Alberta, Canadá (2002). Composting benefits and disadvantages, 2002. Available on <http://www1.agric.gov.ab.ca/$department/deptdocs.nsf/all/eng4464>.

E. Öner, Prof. Dr. (2007). Uzaktan Egitim Platformu (UEP), 2007. Avaliable on <http://www.uzaktanegitimplatformu.com/UEP/uep_ylisans/ey2/ey2_download/Practice%20Guide_Section%202_TGA.pdf>.

A. Paethanom and K. Yoshikawa (2012). Influence of Pyrolysis Temperature on Rice Husk Char Characteristics and Its Tar Adsorption Capability. Energies 5, 2012, 4941-4951.

M. A. Paisley (1998). Battelle future energy resources corp. gasification process.Energy Performance Workshop for the Chemical and Pulp and Paper Industries. US Department of Energy, 1998, pp. 2000–2020.

Parr (Parr Instrument Company) (2007). Introduction to Bomb Calorimetry, 2007. Available on <http://www.scimed.co.uk/wp-content/uploads/2013/03/Introduction-to-bomb-calorimetry.pdf>.

P. Pérez, P. M. Aznar, M. A. Caballero, J. Gil, J. A. Martín and J. Corella (1997). Hot gas cleaning and upgrading with a calcined dolomite located downstream a biomass fluidized bed gasifier operating with steam-oxygen mixtures. Energy & Fuel 11, 1997, 1194-202.

A. F. Plante, J. M. Fernández and J. Leifeld (2009). Application of thermal analysis techniques in soil science. Geoderma 153, 2009, 1–10.

E. Pongrácz, M. Hyvärinen, S. Pitkäaho and R. L. Keiski (2010). Clean air research at the University of Oulu. Proceeding of the SkyPro conference, June 3rd, 2010, University of Oulu, Finland. Kalevaprint, Oulu. ISBN 978-951-42-6199-2, pp.122-125.

N. Popovic (2000). Physical and Chemical Characterization and Upgrading of Char Derived from Scrap Tires by Ultra-Fast Pyrolysis. Thesis (M.Sc.), Memorial University of Newfoundland St. John's, Newfoundland, Canada, 2000.

Proparco, Groupe Agence Française de Développement. Waste: the challenges facing developing countries, 2012. Sources: The World Bank, 2012; GTZ/CWG, 2007; UN Habitat, 2010; Chalmin, P., Gaillochet, C., 2009. Available on <http://www.proparco.fr/jahia/webdav/site/proparco/shared/PORTAILS/Secteur_prive_developpement/PDF/SPD15/SPD15_key_data_uk.pdf>.

C. S. Psomopoulos, A. Bourka and N. J. Themelis (2009). Waste-to-energy: a review of the status and benefits in USA. Waste Management 29, 2009, 1718-1724.

A. J. Ragauskas (2014). Pyrolysis Char Heating Values. Georgia Tech Renewable Bioproducts Institute, 2014. Available on <http://www.ipst.gatech.edu/faculty/ragauskas_art/technical_reviews/char%20bio-oil%20HHV.pdf>.

H. Romar, K. Pieniniemi, P. Tynjälä and U. Lassi (2010). Sampling and determination of tars in biomass-derived product gas. ISBN 978-951-42-6199-2, pp.122-125.

J. G. Ryu, H. Kim, M. H. Kim and J. W. Lee (2004). Morphology and mechanical properties of LDPE/PS blends prepared by ultrasound-assisted melt mixing. Korea-Australia Rheology Journal 16, 2004, 147-152.

SAEM Thales (Sociedad Andaluza de Educación Matemática Thales) (2001). Recursos Didácticos, 2001. Available on <http://thales.cica.es/rd/Recursos/rd99/ed99-0226-01/capitulo4a.html>.

S. Salem K. (2009). Removal of tar in biomass gasification process using carbon materials. Brno University of Technology (BUT), Czech Republic. Chemical Engineering Transactions 18, 2009.

O. Schultz, A. Mette, R. Preu and S.W. Gunz (2007). Silicon solar cells with screen-printed front side metallization exceeding 19% efficiency. Proceedings of the 22nd European Photovoltaic Solar Energy Conference (PVSEC), Milano, 2007. ISBN 3-936338-22-1, pp.980-983.

W. J. Sichina, Marketing Manager of PerkinElmer instruments (2006). Characterization of Polymers Using TGA, 2006. Available on <http://depts.washington.edu/mseuser/Equipment/RefNotes/TGA_Notes.pdf>.

P. A. Simell, N. A. K. Hakala, H. Heikki (1997). Catalytic decomposition of gasification gas tar with benzene as the model compound. Industrial & Engineering Chemistry Research 36, 1997, 42-49.

E. Staniewski (1995). Gasification—The Benefits of Thermochemical Conversion over Combustion. Hazardous Materials Management, 1995.

Ta-Chuang, L. Chang and R. A. Glenn (2006). Gas chromatographic methods developed on the BCR two-stage supper pressure gasification program. Bituminous Coal Research, Inc. 2006. Available on <https://web.anl.gov/PCS/acsfuel/preprint%20archive/Files/12_3_ATLANTIC%20CITY_09-68_0001.pdf>.

C. Unger and M. Ising (2002). Mechanismen und Bedeutung der Teerbildung Teerbeseitigung und bei der termochemischen Umwandlung Kohlenstoffträger fester. Velen, Westphalia. DGMK-Tagungsbericht 2, 2002, 131-142.

VADEB (Vandenbroek International) (2012). Waste Drying & Municipal Waste Treatment. When drying is part of your business, 2012. Available on <http://www.vadeb.com/applications/msw-drying-rdf/>.

S. Vyazovkin and N. Sbirrazzuoli (2006). Isoconversional Kinetic Analysis of Thermally Stimulated Processes in Polymers. Macromolecular Rapid Communications 27, 2006, 1515-1532.

M. Wagner and M. R. Zemo (2013). Material Characterization With Complete Compositional Analysis Using Thermogravimetry. American Laboratory, 2013. Available on < http://www.americanlaboratory.com/914-Application-Notes/128889-Material-Characterization-With-Complete-Compositional-Analysis-Using-Thermogravimetry/>.

D. Wang, S. Czernik and E. Chornet (1998). Production of hydrogen from biomass by catalytic steam reforming of fast pyrolysis oils. Energy Fuel 12, 1998, 19-24.

P. T. Williams (2005). Waste treatment and disposal, 2nd edition. John Wiley & Sons Ltd., Chichester, UK, 2005. ISBN 0-470-84912-6.

U. Wolfesberger (2009). First test runs and tar analyses of a low temperature biomass pilot plant. Master Thesis, Vienna University of Technology, 2009.

U. Wolfesberger, I. Aigner and H. Hofbauer (2009). Tar Content and Composition in Producer Gas of Fluidized Bed Gasification of Wood – Influence of Temperature and Pressure. Gas Technology Institute (GTI), tcbiomass, Chicago. Environmental Progress & Sustainable Energy 28, 2009, 372–379.